University Graduate School of Medicine — N. Matsuyoshi; Osaka University Graduate School of Medicine — T. Nakamura; Nara Medical University — H. Niizeki; Wakayama Medical University — T. Kishi; Okayama University Graduate School of Medicine — T. Ohno, G. Nakanishi; Ehime University Graduate School of Medicine — K. Sayama, Y. Shirakata, S. Murakami; Kyushu University Graduate School of Medicine — Y. Moroi, M. Takahara, H. Kuniba, T. Uenotsuchi; Kurume University School of Medicine — N. Momosaki, K. Hashikawa; Oita University Faculty of Medicine — O. Okamoto; University of Occupational and Environment Health — R. Yoshiki, C. Koga, D. Nishio; and Faculty of Medical and Pharmaceutical Sciences, Kumamoto University — S. Wakasugi.

SPECIAL NOTICE REGARDING CASE REPORTS

The *Journal of the American Academy of Dermatology*, like other medical journals, receives many more case reports than we are able to publish. To accommodate our authors and to give our readers access to a more diverse collection of interesting cases, effective January 1, 2009 all case reports must be submitted in the more abbreviated case letter format. A full description of the case letter format can be found in the most recent written and online Instructions for Authors.

Additionally, because of our current high inventory, lengthy delays may occur before already accepted case reports and case letters appear in the print journal. To circumvent this, authors may elect "online-only" publication of their cases. Online-only articles are accessible at http://www.eblue.org. "Online-only" is a bonafide form of publication. Online articles may be listed on the author's curriculum vitae and are cited on PubMed. For further information regarding online publication, please contact Melissa Derby, Managing Editor, at mderby@aad.org.

Bruce H. Thiers, MD, Editor
Dirk M. Elston, MD, Deputy Editor

Journal of Dermatological Science 54 (2009) 38–42

Contents lists available at ScienceDirect

Journal of Dermatological Science

journal homepage: www.intl.elsevierhealth.com/journals/jods

Differentiation of *Trichophyton rubrum* clinical isolates from Japanese and Chinese patients by randomly amplified polymorphic DNA and DNA sequence analysis of the non-transcribed spacer region of the rRNA gene

Xiumin Yang [a,b,c], Takashi Sugita [c,*], Masako Takashima [d], Masataro Hiruma [e], Ruoyu Li [f], Hajime Sudo [a], Hideoki Ogawa [a], Shigaku Ikeda [a]

[a] Department of Dermatology, Juntendo University School of Medicine, Bunkyo-ku, Tokyo 113-8421, Japan
[b] Department of Dermatology, Beijing Tongren Hospital, Affiliate of Capital University of Medical Sciences, Beijing 100730, China
[c] Department of Microbiology, Meiji Pharmaceutical University, Kiyose, Tokyo 204-8588, Japan
[d] Microbe Division/Japan Collection of Microorganisms, RIKEN BioResource Center, Wako, Saitama 351-0198, Japan
[e] Department of Dermatology and Allergy, Juntendo University Nerima Hospital, Nerima-ku, Tokyo 177-0033, Japan
[f] Department of Dermatology and Research Center of Medical Mycology, Peking University First Hospital, Beijing 100034, China

ARTICLE INFO

Article history:
Received 3 June 2008
Received in revised form 7 November 2008
Accepted 7 December 2008

Keywords:
Trichophyton rubrum
RAPD
NTS
rRNA gene
Japan
China

ABSTRACT

Background: *Trichophyton rubrum* is the most common pathogen causing dermatophytosis worldwide. Recent genetic investigations showed that the microorganism originated in Africa and then spread to Europe and North America via Asia.
Objects: We investigated the intraspecific diversity of *T. rubrum* isolated from two closely located Asian countries, Japan and China.
Methods: A total of 150 clinical isolates of *T. rubrum* obtained from Japanese and Chinese patients were analyzed by randomly amplified polymorphic DNA (RAPD) and DNA sequence analysis of the non-transcribed spacer (NTS) region in the rRNA gene.
Results: RAPD analysis divided the 150 strains into two major clusters, A and B. Of the Japanese isolates, 30% belonged to cluster A and 70% belonged to cluster B, whereas 91% of the Chinese isolates were in cluster A. The NTS region of the rRNA gene was divided into four major groups (I–IV) based on DNA sequencing. The majority of Japanese isolates were type IV (51%), and the majority of Chinese isolates were type III (75%).
Conclusions: These results suggest that although Japan and China are neighboring countries, the origins of *T. rubrum* isolates from these countries may not be identical. These findings provide information useful for tracing the global transmission routes of *T. rubrum*.

1. Introduction

Trichophyton rubrum is presently the most common worldwide pathogen causing dermatophytoses such as tinea corporis, tinea capitis, tinea pedis, and onychomycosis [1,2]. The microorganism was thought to have originated as a cause of chronic tinea corporis in the late 19th century from areas of endemicity in Southeast Asia and to have subsequently been spread to Europe and North America by soldiers during the First World War [3]. However, most recent investigations indicate that the *T. rubrum* complex originated in Africa and that a new genotype subsequently emerged in Asia and spread to Europe and the United States [4]. Such epidemiological investigations depend on advances in molecular techniques. Randomly amplified polymorphic DNA (RAPD) and restriction fragment length polymorphism (RFLP) analyses can distinguish closely related species or strains. In the case of *Trichophyton*, RAPD analysis can distinguish *T. rubrum* or *Trichophyton mentagrophytes* at the level of the strain or genotypic group [5–9]. The RFLP method has also been used to identify several types of *T. rubrum* [10,11].

In both Japan and China, approximately 80% of dermatophytosis patients are infected by *T. rubrum* [12,13]. In an epidemiological survey of *T. rubrum* clinical isolates from Japanese and Chinese dermatophytosis patients, we found that the isolates, although closely related, were genetically different. In this paper, we report a molecular epidemiological investigation of *T. rubrum* clinical isolates obtained from Japanese and Chinese patients, using RAPD analysis and DNA sequence analysis of rDNA.

* Corresponding author. Tel.: +81 424 95 8762; fax: +81 424 95 8762.
E-mail address: sugita@my-pharm.ac.jp (T. Sugita).
Abbreviations. bp, pase pairs; RAPD, randomly amplified polymorphic DNA; NTS, non-transcribed spacer.

0923-1811/$30.00
doi:10.1016/j.jdermsci.2008.12.009

2. Materials and methods

2.1. Fungal strains

This study examined 150 *T. rubrum* clinical isolates, of which 85 were isolated in Tokyo and the neighboring prefectures in Japan, and 65 were isolated in Beijing, China. All isolates were identified as *T. rubrum* by DNA sequence analysis of the internal transcribed spacer (ITS) region of the rRNA gene [14].

2.2. Extraction of fungal DNA

All isolates were grown on Sabouraud dextrose agar and incubated at 25 °C for 7 days. DNA was extracted with an ISOPLANT kit (Nippon Gen Co. Ltd., Toyama, Japan) according to the manufacturer's instructions. The DNA concentration of each sample was measured using Nano Drop (Thermo Fisher Scientific, GA, USA).

2.3. Genotyping the non-transcribed spacer (NTS) region in the rRNA gene

The partial DNA sequence of the NTS region, which is located between the 26S and 18S subunits of the rRNA gene, was determined. The forward (TR-F, 5′-AGA AGA TCT ACA CAG ATA CTA TC-3′) and reverse (TR-R, 5′-TAC ATA TAC TCA CCG AGG TCT GT-3′) primers were designed with reference to gene sequences in GenBank (accession numbers AF222890 and AF222888). Amplifications were performed in a total volume of 50 μl containing 5 μl of 10× PCR buffer [100 mM Tris–Cl (pH 8.3), 500 mM KCl, 20 mM $MgCl_2$; Takara Bio, Shiga, Japan], 4 μl of 200 μM deoxynucleoside triphosphate (equimolar dNTPs), 20 pmol of each primer, 1.25 U of Takara EX *Taq* DNA polymerase (Takara Bio), and 100 ng of fungal DNA. PCR consisted of an initial denaturation at 94 °C for 1 min, followed by 30 cycles of 30 s at 94 °C, 30 s at 50 °C, and 1 min at 72 °C, with a final 10-min extension at 72 °C. The partial NTS regions were sequenced using four primers (TR-F, TR-R, TR-F2 (5′-CCGCATCTCTGCAAGGCCT-3′), and TR-R2 (5′-AGGCCTTGCAGA-GATGCGG-3′)) and a BigDye Terminator Cycle Sequencing Ready Reaction kit version 3.1 (PerkinElmer Applied Biosystems, Foster City, CA, USA), according to the manufacturer's instructions.

2.4. RAPD analysis

Two decamer primers (No. 1, GGTGCGGGAA; No. 6, CCCGTCAGCA) were used as a single primer in the RAPD analysis [9]. A preliminary investigation was carried out to determine reactivity and reproducibility of the RAPD method. As the reaction parameters are critical for primer binding, we also optimized the PCR conditions. Amplifications were performed in a total volume of 50 μl containing 5 μl of 10× PCR buffer [100 mM Tris–HCl (pH 8.3), 500 mM KCl, 15 mM $MgCl_2$; Nippon Gene Co., Toyama, Japan], 4 μl of 200 μM deoxynucleoside triphosphate (equimolar dNTPs; Nippon Gene Co.), 30 pmol of each primer, 200 ng of fungal DNA, and 2.5 U of Gene *Taq* FP DNA polymerase (Nippon Gene Co.), which was specifically developed for RAPD analysis. PCR was performed with an initial denaturation at 94 °C for 3 min, followed by 40 cycles of 30 s at 94 °C, 60 s at 36 °C, and 60 s at 72 °C, with a final extension at 72 °C for 10 min. The amplification products were separated by 1.5% agarose gel electrophoresis in 1× Tris–acetate/EDTA buffer. Each DNA fragment was scored as present or absent. The intensities of the PCR fragments were not measured. A phenogram showing the similarities of the isolates was generated using the unweighted pair group method with arithmetic mean (UPGMA phenogram), based on the pairwise similarity coefficient matrix. The program Phylogenetic Analysis Using Parsimony (PAUP, version 4.0b2; David L. Swofford, Laboratory of Molecular Systematics, National Museum of Natural History, Smithsonian Institution, Washington, DC, USA) was used to calculate similarity values and to generate the UPGMA phenogram.

3. Results

3.1. Genotyping the NTS region

Fragments of the NTS region that were 811–1213 bp in length were amplified. They were divided into four major genotypes according to length: 811 bp (I), 911 bp (II), 1011 bp (III), and 1211–1213 bp (IV). Each genotype was further divided into subtypes with several nucleotide substitutions, as shown in Table 2. Of the 85 Japanese isolates, the majority were genotype IV (50.6%, 43/85), followed by genotype III (30.6%, 26/85), genotype II (12.9%, 11/85), and genotype I (5.9%, 5/85). The major Chinese isolate was genotype III (75.4%, 49/65), followed by II (15.4%, 10/65) and IV

Table 1
Fingerprinting genotype of the *Trichophyton rubrum* clinical isolates.

Cluster	Subcluster	Fingerprinting genotype[a] according to primer															
		Primer 1									Primer 6						
A		200[b]	250	300	350	400	500	550	600	700	250	300	400	500	600	700	800
	1	0	0	1	0	1	1	0	1	0	0	1	0	1	0	1	0
	2	0	0	1	0	1	1	0	0	0	0	1	0	1	0	1	0
	3	0	0	1	0	1	1	0	0	1	0	1	0	1	0	1	0
	4	0	0	1	0	1	1	0	1	1	0	1	0	1	0	1	0
	5	0	0	0	0	0	1	0	1	0	0	1	0	1	0	1	0
	6	0	0	0	0	1	1	0	1	0	0	1	0	1	0	1	0
	7	0	0	0	1	1	1	0	1	0	0	1	0	1	0	1	0
	8	0	0	0	0	1	1	0	1	1	0	1	0	1	0	1	0
	9	0	0	1	0	1	0	0	0	0	0	1	0	1	0	1	0
	10	0	0	1	0	0	0	0	1	0	0	1	0	1	0	1	0
	11	0	0	0	0	0	0	1	0	0	0	1	0	1	0	1	0
	12	0	0	0	1	0	0	0	0	0	0	1	0	1	0	1	0
	13	0	1	0	0	0	1	0	0	0	0	1	0	1	0	1	0
	14	0	0	0	1	1	1	1	0	0	0	1	0	1	0	1	0
B	1	0	0	1	0	1	1	0	1	0	0	0	0	0	1	0	1
	2	0	0	1	0	1	1	0	1	0	1	0	1	0	1	0	1
	3	0	0	1	0	1	1	0	0	0	1	0	1	0	0	0	0
	4	1	0	1	0	1	1	0	1	0	0	0	0	0	0	0	0
	5	1	0	1	0	1	1	0	1	0	0	0	1	0	0	0	0

[a] 1, PCR product present; 0, fragment absent.
[b] Length (bp) of PCR product.

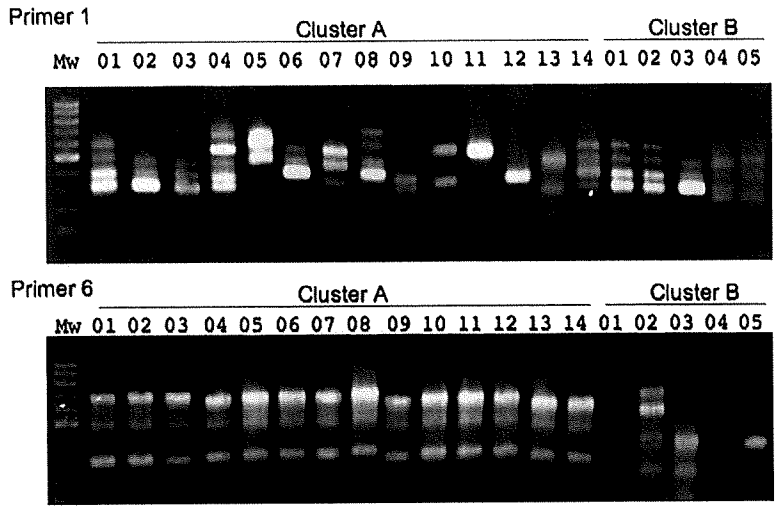

Fig. 1. Representative electrophoresis gel of PCR fingerprints obtained from *Trichophyton rubrum* isolates using primers No. 1 and No 6. Mw, Molecular weight marker, 100 bp ladder.

(9.2%, 6/65). Genotype I was not detected in China. The nucleotide sequences of these subtypes were deposited in GenBank as AB437940 (Ia), AB438033 (Ib), AB438034 (Ic), AB437941 (II), AB437942 (IIIa), AB438035 (IIIb), AB438036 (IIIc), AB438037 (IIId), AB438038 (IIIe), AB438039 (IIIf), AB438040 (IIIg), AB437943 (IVa), AB438041 (IVb), AB437944 (IVc), AB438042 (IVd), AB438043 (IVe), and AB438044 (IVf).

3.2. RAPD analysis

The two decamer primers, No. 1 and No. 6, produced nine (approximately 200, 250, 300, 350, 400, 500, 550, 600, and 700 bp) and seven polymorphic bands (approximately 250, 300, 400, 500, 600, 700, and 800 bp), respectively (Table 1). Representative electrophoresis of each fingerprins is also shown in Fig. 1. The resulting UPGMA phenogram consisted of two major clusters, A and B (Fig. 2). Clusters A and B were further divided into 14 subclusters with 85 strains and five subclusters with 65 strains, respectively (Fig. 1 and Tables 1 and 2). Of the 85 Japanese strains, 26 (30.1%, 26/85) were in cluster A and 59 (69.4%, 59/85) were in cluster B. The major subclusters of clusters A and B were 1 (92.3%, 24/26) and 2 and 3 (83.0%, 49/59), respectively. Of the 65 Chinese strains, most were distributed in cluster A (90.7%, 59/65) and subcluster 1 (41/59). Only six strains (9.3%) were in cluster B.

3.3. Relationship between NTS genotypes and RAPD profiles

Of the four NTS genotypes, genotypes I, III, and IV corresponded to specific clusters identified via RAPD analysis. NTS genotype III was only identified in a strain within cluster A, and NTS genotypes I and IV were only identified in strains within cluster B. In contrast, NTS genotype II was found in strains within both clusters.

Table 2
Genotype of the NTS region of the rRNA gene of Japanese and Chinese clinical isolates of *T. rubrum*.

Cluster	Subcluster	Japanese isolates																	Chinese isolates														Total
		Genotype																	Genotype														
		I			II	III							IV						Subtotal	I			II	III							IV						Subtotal	
		a	b	c	a	a	b	c	d	e	f	g	a	b	c	d	e	f		a	b	c	a	a	b	c	d	e	f	g	a	b	c	d	e	f		
A	1							1	1	1	1	20							24					4	16	14	3	4									41	65
	2					2													2						3	1											4	6
	3																		0							2											2	2
	4																		0											2							2	2
	5																		0				1														1	1
	6																		0				1														1	1
	7																		0				1														1	1
	8																		0				1														1	1
	9																		0				1														1	1
	10																		0				1														1	1
	11																		0				1														1	1
	12																		0				1														1	1
	13																		0				1														1	1
	14																		0				1														1	1
	Subtotal	0			0	26							0						26	0			10	49							0						59	85
B	1	1																	1																		0	1
	2				4								2					23	29													1	1	1	1	1	1	6	35
	3				2													18	20																		0	20
	4	1			2														3																		0	3
	5	1	1	1	3														6																		0	6
	Subtotal	5			11	0							43						59	0			0	0							6						6	65
	Total	5			11	26							43						85	0			10	49							6						65	150

Fig. 2. UPGMA phenogram of *Trichophyton rubrum* isolates calculated from the DNA fingerprinting patterns obtained with primers No. 1 and No. 6.

4. Discussion

Several tools have been developed to identify strains of *T. rubrum* using molecular methods [5,6,15]. Jackson et al. [16] first introduced a useful analysis for *T. rubrum* strain identification using the NTS region of the rRNA gene. The *T. rubrum* NTS region contains two tandem repeat sequences (TRSs): TRS-1, which comprises a 27-bp palindromic sequence, and TRS-2. TRS-1 gave 21 PCR types, and 23 separate PCR types were recognized upon amplification of both TRS-1 and TRS-2. The PCR type was not correlated with the clinical specimen but appeared to show a bias in geographic distribution. Since Jackson et al. introduced the structure of the NTS region [16], the NTS region has been widely used for epidemiological studies of not only *T. rubrum* but also other *Trichophyton* species such as *Trichophyton tonsurans* [17–19] and *Trichophyton violaceum* [20]. The NTS sequences of *T. rubrum* and *T. violaceum* share 85% similarities and both contain TRS-1 and TRS-2 [20]. In this study, we designed new PCR primers that amplify the region between nucleotides 811 and 1213, which includes TRS-1, and determined this sequence in 150 *T. rubrum* strains. RAPD is the most commonly used method for epidemiological studies or strain typing of fungi. The proper selection of primers is critical in the RAPD method. Baeza et al. [9] indicated that strains could be differentiated using a combination of RAPD patterns with two decamer oligonucleotide primers, No. 1 and No. 6. To increase accuracy, we performed DNA sequencing of the TRS-1 region in addition to PCR genotyping in the present study. The NTS genotype II strains were found in both of the major clusters that were identified via RAPD profiling, whereas the remaining NTS genotypes (I, III, and IV) were associated with only one specific cluster. Although there may be exceptions given that this is an epidemiological study, the NTS genotypes and RAPD profiles determined in the present study were not randomly distributed between countries. The combination of NTS genotyping and RAPD profiling revealed that the Japanese and Chinese strains differed in terms of the predominant NTS genotype and RAPD profile, allowing the identification of a characteristic *T. rubrum* from each country. RAPD profiles constructed from the decamer primers used in this study correlated well with the analytical results obtained from TRS-1 sequencing.

One aim of this study was to investigate the intraspecific diversity of *T. rubrum* isolated from Japan and China. Microsatellite (GT)8–10 diversity analysis has suggested that *T. rubrum* (genotype A) is of African origin and later spread to North America and Europe via Asia [4]. In Asia, the new genotype B appeared and subsequently spread to North America and Europe. Ohst et al. [4] reported that genotype A and B strains occurred with nearly equal frequency, even within the limited region of Ishikawa prefecture. We found that the Japanese isolates were divided into four main types, based on RAPD profiles. We did not perform microsatellite (GT)8–10 diversity analysis in this study, but such an investigation would provide further useful information in combination with our current results. We cannot comment on the worldwide distribution or transmission of *T. rubrum*, as we did not examine strains from other countries in Asia, North America, or Europe. It is interesting that the intraspecific diversity of microorganisms obtained from Japan and China differed, despite the long history of exchange between the two countries.

In conclusion, we found that the *T. rubrum* clinical isolates obtained from Japan and China were genetically different, although the two countries are in geographical proximity. In future studies using strains from multiple nations, the combination of RAPD with two decamer primers and NTS sequencing may enable the elucidation of the worldwide transmission routes of *T. rubrum*.

Conflict of interest

None to declare.

Acknowledgement

Xiumin Yang is partially supported by the Japan International Cooperation Agency.

References

[1] Evans EG. Causative pathogens in onychomycosis and the possibility of treatment resistance: a review. J Am Acad Dermatol 1998;38:S32–6.
[2] Borman AM, Campbell CK, Fraser M, Johnson EM. Analysis of the dermatophyte species isolated in the British Isles between 1980 and 2005 and review of worldwide dermatophyte trends over the last three decades. Med Mycol 2007;45:131–41.
[3] Rippon JW. Medical mycology: the pathogenic fungi and pathogenic *Actiomycetes*. Philadelphia, PA: W.B. Saunders Co.; 1988. p. 169–182.
[4] Ohst T, de Hoog S, Presber W, Stavrakieva V, Graser Y. Origins of microsatellite diversity in the *Trichophyton rubrum–T. violaceum* clade (Dermatophytes). J Clin Microbiol 2004;42:4444–8.
[5] Mochizuki T, Sugie N, Uehara M. Random amplification of polymorphic DNA is useful for the differentiation of several anthropophilic dermatophytes Mycoses 1997;40:405–9.
[6] Graser Y, Kuhnisch J, Presber W. Molecular markers reveal exclusively clonal reproduction in *Trichophyton rubrum*. J Clin Microbiol 1999,37:3713–7.
[7] Kac G, Bougnoux ME, Feuilhade De Chauvin M, Sene S, Derouin F. Genetic diversity among *Trichophyton mentagrophytes* isolates using random amplified polymorphic DNA method. Br J Dermatol 1999;140:839–44.
[8] Kim JA, Takahashi Y, Tanaka R, Fukushima K, Nishimura K, Miyaji M. Identification and subtyping of *Trichophyton mentagrophytes* by random amplified polymorphic DNA. Mycoses 2001;44:157–65.
[9] Baeza LC, Matsumoto MT, Almeida AM, Mendes-Giannini MJ. Strain differentiation of *Trichophyton rubrum* by randomly amplified polymorphic DNA and analysis of rDNA nontranscribed spacer. J Med Microbiol 2006;55:429–36.
[10] Gupta AK, Kohli Y, Summerbell RC. Variation in restriction fragment length polymorphisms among serial isolates from patients with *Trichophyton rubrum* infection. J Clin Microbiol 2001;39:3260–6.
[11] Kanbe T, Suzuki Y, Kamiya A, Mochizuki T, Kawasaki M, Fujihiro M, et al. Species-identification of dermatophytes *Trichophyton, Microsporum* and epidermophyton by PCR and PCR-RFLP targeting of the DNA topoisomerase II genes. J Dermatol Sci 2003;33:41–54.
[12] Chinese Collaborative Fungi Research Group. Epidemiological study of pathogenic fungi in China: 1986 and 1996. Chin Med J 2001;114:294–6
[13] Nishimoto K. An epidemiological survey of dermatomycoses in Japan, 2002. Nippon Ishinkin Gakkai Zasshi 2006;47:103–11.
[14] Makimura K, Tamura Y, Mochizuki T, Hasegawa A, Tajiri Y, Hanazawa R, et al. Phylogenetic classification and species identification of dermatophyte strains based on DNA sequences of nuclear ribosomal internal transcribed spacer 1 regions. J Clin Microbiol 1999;37:920–4.
[15] Yang G, An L, Li Q, Lin J, Liu W, Jin L, et al. Genotyping of *Trichophyton rubrum* by analysis of ribosomal-DNA intergenic spacer regions. Mycopathologia 2007;164:19–25.
[16] Jackson CJ, Barton RC, Kelly SL, Evans EG. Strain identification of *Trichophyton rubrum* by specific amplification of subrepeat elements in the ribosomal DNA nontranscribed spacer. J Clin Microbiol 2000;38:4527–34.
[17] Gaedigk A, Gaedigk R, Abdel-Rahman SM. Genetic heterogeneity in the rRNA gene locus of *Trichophyton tonsurans*. J Clin Microbiol 2003;41:5478–87
[18] Sugita T, Shiraki Y, Hiruma M. Genotype analysis of the variable internal repeat region in the rRNA gene of *Trichophyton tonsurans* isolated from Japanese Judo practitioners. Microbiol Immunol 2006;50:57–60.
[19] Mochizuki T, Kawasaki M, Tanabe H, Anzawa K, Ishizaki H, Choi JS Molecular epidemiology of *Trichophyton tonsurans* isolated in Japan using RFLP analysis of non-transcribed spacer regions of ribosomal RNA genes. Jpn J Infect Dis 2007;60:188–92.
[20] Chang JC, Hsu MM, Barton RC, Jackson CJ. High-frequency intragenomic heterogeneity of the ribosomal DNA intergenic spacer region in *Trichophyton violaceum*. Eukaryotic Cell 2008;7:721–6.

Biochemical and Biophysical Research Communications 388 (2009) 102–106

Contents lists available at ScienceDirect

Biochemical and Biophysical Research Communications

journal homepage: www.elsevier.com/locate/ybbrc

Involvement of PU.1 in the transcriptional regulation of TNF-α

Tatsuo Fukai [a,b], Chiharu Nishiyama [a,*], Shunsuke Kanada [a], Nobuhiro Nakano [a], Mutsuko Hara [a], Tomoko Tokura [a], Shigaku Ikeda [a,b], Hideoki Ogawa [a], Ko Okumura [a]

[a] Atopy (Allergy) Research Center, Juntendo University School of Medicine, 2-1-1 Hongo, Bunkyo-ku, Tokyo 113-8421, Japan
[b] Department of Dermatology, Juntendo University School of Medicine, 2-1-1 Hongo, Bunkyo-ku, Tokyo 113-8421, Japan

ARTICLE INFO

Article history:
Received 22 July 2009
Available online 30 July 2009

Keywords:
PU.1
Transcription factor
TNF-α
Dendritic cells
Mast cells

ABSTRACT

PU.1 is a myeloid- and lymphoid-specific transcription factor that serves many important roles in the development and specific gene regulation of hematopoietic lineages. Mast cells (MC) and dendritic cells (DC) express PU.1 at low and high levels, respectively. Previously, we found that enforced expression of PU.1 in MC resulted in acquisition of DC-like characteristics, including repression of several IgE-mediated responses due to reduced expression of IgE-signaling related molecules. In contrast, PU.1 overexpression in MC up-regulated TNF-α production in response to IgE- and LPS-stimulation suggesting that PU.1 positively regulates TNF-α expression. However, the role of PU.1 in the expression of TNF-α is largely unknown. In the present study, the effects of PU.1 on the TNF-α promoter in mouse bone marrow-derived (BM) MC and DC were studied. Real-time PCR, ELISA, and chromatin immunoprecipitation assays indicated that the kinetics and magnitude of TNF-α expression levels following LPS- or IgE-stimulation are related to the amount of PU.1 binding to the promoter. In brief, higher and delayed up-regulation of TNF-α promoter function was observed in DC, whereas there were lower and rapid responses in MC. When PU.1-overexpressing retrovirus vector was introduced into MC, the amount of PU.1 recruited to the TNF-α promoter markedly increased. The knockdown of PU.1 in BMDC by siRNA resulted in a reduction of TNF-α protein produced from LPS-stimulated BMDC. These observations indicate that PU.1 transactivates the TNF-α promoter and that the amount of PU.1 binding on the promoter is associated with promoter activity.

Introduction

The transcription factor, PU.1 belongs to the Ets-family, which possesses the Ets-domain as a DNA-binding region. PU.1 is involved in the development and specific gene regulation of the myeloid- and lymphoid-lineages, including macrophages, dendritic cells (DC), neutrophils, mast cells (MC), and lymphoid cells [1–7].

Although PU.1 is involved in specific gene expression in MC [7,8], the level of PU.1 expression itself is lower in MC than that in monocytes, including DC [9]. We previously found that enforced expression of PU.1 in MC or its progenitors induces various monocyte (DC-like)-characteristics, including specific gene expression and morphological changes [10–12]. This suggests that the level of PU.1 expression determines cell fate between MC and DC. MC that overexpress PU.1 exhibit enhanced expression of LPS-mediated cytokine production [10–13]. Although several IgE-mediated responses are suppressed by PU.1 overexpression, TNF-α production increases in response to IgE-stimulation as well as LPS-stimulation. These studies indicate that PU.1 may up-regulate the signaling pathway under TLR4 and/or that PU.1 may transactivate the TNF-α promoter in a stimulation-independent manner. Although PU.1 is reported to recognize the essential element in the TLR4 promoter [14] and to control alternative TLR4 promoter usage [15], overexpression of PU.1 does not affect the surface TLR4 expression level on MC [12]. In addition, the TLR4-signaling pathway was not identified through clustering analysis of microarray data, whereas the FcεRI-signaling pathway was significantly down-regulated in MC that overexpress PU.1 [13]. Based on these observations, we hypothesized that PU.1 directly transactivates the TNF-α promoter. Although several studies of the structure of the TNF-α promoter have been reported [16–19], the role of PU.1 in TNF-α promoter function is largely unknown.

In the present study, the involvement of PU.1 in TNF-α promoter function was analyzed. TNF-α expression levels were measured using ELISA and RT-PCR, and PU.1 recruitment to the promoter was monitored using the chromatin immunoprecipitation

Abbreviations: BM, bone marrow-derived; ChIP, chromatin immunoprecipitation; DC, dendritic cell; MC, mast cell.

* Corresponding author. Fax: +81 3 3813 5512
E-mail address: chinishi@juntendo.ac.jp (C. Nishiyama).

0006-291X/$ - see front matter © 2009 Elsevier Inc. All rights reserved.
doi:10.1016/j.bbrc.2009.07.126

(ChIP) assay. This was conducted under various conditions of the cells, in which PU.1 was overexpressed by infection with retrovirus carrying PU.1 cDNA, or in which PU.1 expression was knocked down by introduction of PU.1 siRNA.

Materials and methods

Cells. To generate BMMC, BM cells prepared from BALB/c mice (Japan SLC, Hamamatsu, Japan) were grown in RPMI 1640 medium (Sigma–Aldrich) supplemented with 10% heat-inactivated FBS, 100 μM 2-ME, 10 μM MEM nonessential amino acids solution (Sigma–Aldrich), 100 U/ml penicillin, 100 μg/ml streptomycin, and pokeweed mitogen-stimulated spleen-condition medium (PWM-SCM) [20] for 3–5 weeks, as previously described [12]. BMDC were prepared from BALB/c BM cells with culture in RPMI 1640 supplemented with 10% FBS, 100 μM 2-ME, 10 μM MEM nonessential amino acids solution, antibiotics, and 10 ng/ml mouse rGM-CSF (PeproTech) based on a previously reported method [21].

LPS and IgE stimulation. LPS (from *Escherichia coli*; Sigma–Aldrich) was used to stimulate BMMC or BMDC via TLR4. Stimulation of BMMC via FcεRI was performed with mouse anti-DNP-IgE (BD Pharmingen) and anti-mouse IgE (R35–72; BD Pharmingen) as described previously [13,22].

Quantification of mRNA by real-time PCR. Total RNA prepared from BMMC or BMDC using an RNeasy Micro Kit (QIAGEN) was reverse transcribed with a High Capacity cDNA Reverse Transcription Kit (Applied Biosystems, Foster City, CA). The amount of mRNA of TNF-α, PU.1, and GAPDH was quantified using a 7500 Real-Time PCR System (Applied Biosystems) with TaqMan Gene Expression Assays (Applied Biosystems; #Mm00443258_m1 for TNF-α, #Mm00488140 for PU.1, and rodent GAPDH #4308313) and TaqMan Universal Master Mix (Applied Biosystems). Each expression level of TNF-α or PU.1 was defined as the ratio to GAPDH by calculating the cycle threshold (Ct) values in amplification plots using 7500 SDS software as described previously [23].

Determination of TNF-α production level by ELISA. The amount of TNF-α protein in culture medium was measured using a Quantikine ELISA Kit (R&D Systems) [13].

Chromatin immunoprecipitation (ChIP) assay. The ChIP assay was performed as previously described [24,25]. Anti-PU.1 goat IgG (#D-19, #sc-5949, Santa Cruz Biotechnology) and goat IgG (#02-6202, Invitrogen) were used. Chromosomal DNA was quantified with a 7500 Rea-Time PCR System using the following synthesized primers and TaqMan probes (Applied Biosystems): for TNF-α promoter (−132/−71), forward primer TNF-α-132F (5′-CCGCTTCCTCCACATG AGA-3′), reverse primer TNF-α-71R (5′-TCATTCAACCCTCGGAAAA CTT-3′), and TaqMan probe TNF-α-112P (5′-FAM-CATGGTTTTCTCC ACCAAG-MGB-3′).

PU.1 overexpression with retrovirus vector. Retrovirus vector carrying PU.1 cDNA and its mock vector were generated by transfection of packaging cells Plat-E with plasmids pMXs-puro-PU.1 [13] and pMXs-puro, respectively. BMMC was then transfected with each retrovirus vector and maintained in the presence of puromycine to select transfectants as described previously [10,12,13].

siRNA-mediated inhibition of PU.1 expression. PU.1 siRNA (Stealth Select RNAi, #MSS247676) and control siRNA (Stealth RNAi Negative Universal Control, #45-2001) were purchased from Invitrogen. A 5 μl aliquot of 20 μM siRNA was introduced into 1×10^5 BMDC with a Mouse Macrophage Nucleofector Kit (Amaxa GbmH, Koeln, Germany) using Nucleofector II (Amaxa) set at Y-001 as described in our previous reports [24,26].

Results

Transcription kinetics of TNF-α in BMDC and BMMC

In order to analyze the kinetics of the transcription levels, the amount of TNF-α mRNA in BMDC and BMMC was measured at various time points following LPS or IgE stimulation. The level of TNF-α mRNA in LPS-stimulated BMDC reached a maximum at 1 h post-stimulation of approximately 70-fold that of the control cell level without stimulation (**Fig. 1**A, left). In IgE-stimulated BMMC, the level of TNF-α mRNA rapidly increased to a maximum value at 30 min of approximately 30-fold that of control cell level and then markedly decreased to 3 h post-stimulation (**Fig. 1**A, right). In LPS-stimulated BMMC, the level of TNF-α mRNA increased by 2.5-fold that of the control cell level; a much smaller increase than those seen in the LPS-stimulated BMDC and IgE-stimulated BMMC (**Fig. 1**A, middle). These results suggest that TNF-α transcription rapidly peaked and then decreased to the basal level in IgE-stimulated BMMC in contrast to sustained up-regulation in LPS-stimulated BMDC.

At the same time, the concentration of TNF-α in the culture medium released from cells was also measured (**Fig. 1**B). The TNF-α concentration released from DC was markedly higher than that from either IgE-stimulated MC or LPS-stimulated MC, while LPS-stimulated BMDC showed the highest response. Conversely, the concentration of TNF-α released from LPS-stimulated BMMC was the lowest, indicating that the kinetics and magnitude of TNF-α protein production from stimulated cells are somewhat affected by transcriptional regulation.

Specific binding of PU.1 to the TNF-α promoter in BMDC and BMMC

A ChIP assay was performed to examine whether PU.1 binds to the TNF-α promoter regions on chromosomal DNA in BMDC and BMMC. As shown in **Fig. 2**A, the amount of chromosomal DNA around the TNF-α promoter immunoprecipitated with anti-PU.1 Ab was significantly higher than that with control Ab in non-stimulated BMDC or BMMC. The relative input unit of specific binding of PU.1 in BMDC (**Fig. 2**A, left) was higher than those in LPS- and IgE-stimulated BMMC (**Fig. 2**A, middle and right, respectively). The PU.1-binding level on the promoter was transiently up-regulated following LPS- or IgE-stimulation reaching a maximum value at 30 min post-stimulation in LPS-stimulated BMDC, and at 15–30 min in LPS- or IgE-stimulated BMMC, and rapidly decreased to control cell levels at 60 min post-stimulation in BMMC. In contrast, the increased binding remained present at 60 min post-stimulation in BMDC. Such significant binding of PU.1 was not observed when a non-related control region was analyzed (data not shown). These results indicate that PU.1 constitutively binds the TNF-α promoter in BMDC and BMMC and that the amount of PU.1 binding to these promoters parallels the expression magnitude and kinetics. When the PU.1-binding motifs GGAA and AGAA [8] were searched for in the promoter region, nine motifs were found in 200 bp of the TNF-α promoter, which include the essential elements required for LPS- or cytomegalovirus-induced activation in a monocytic cell line [16–19] (**Fig. 2**B). Therefore, PU.1 may bind the promoter region via these multiple motifs.

Occupancy of the TNF-α promoter by PU.1 in PU.1-overexpressing MC

When PU.1 was overexpressed in BMMC, LPS-induced TNF-α production dramatically increased and reached the same level of production as that from BMDC [13]. Considering the present results, the occupancy of the TNF-α promoter with PU.1 may have been increased by enforced expression of PU.1. To confirm this

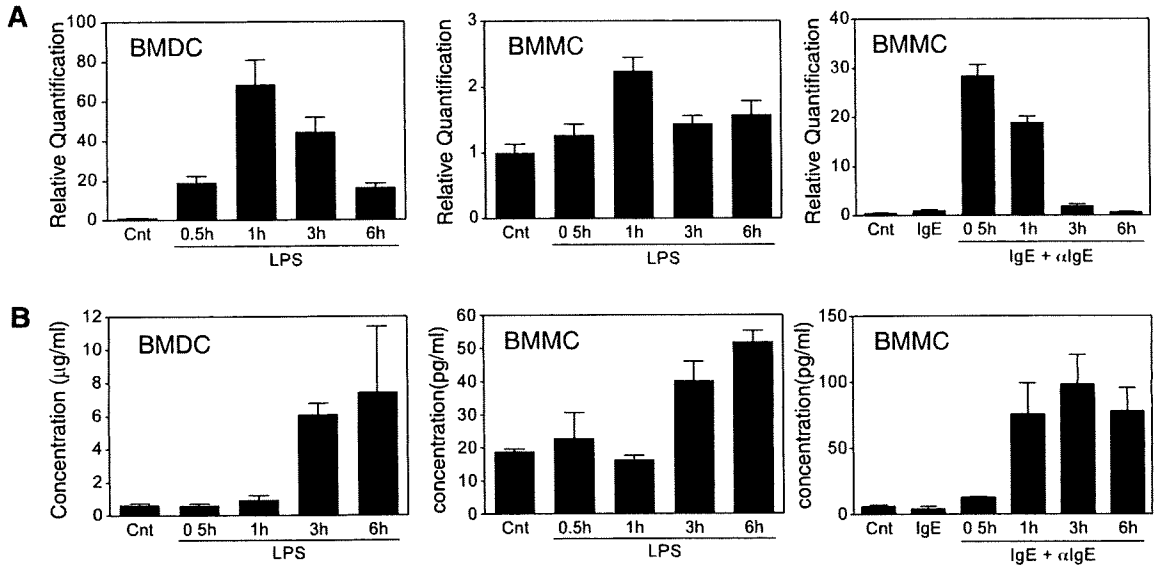

Fig. 1. TNF-α expression levels in stimulated BMDC and BMMC. (A) Fold increase of TNF-α mRNA in LPS- or IgE-stimulated BMDC and BMMC. Messenger RNA levels of TNF-α normalized against GAPDH are presented as the ratio to that without LPS (left and middle) or to that of IgE alone without anti-IgE Ab (right). Data represent average ± SD of triplicate samples. A representative result from three independent experiments is shown. Cnt: control cells without any additives for stimulation in all figures. (B) The concentration of TNF-α protein released from stimulated BMDC and BMMC. Data represent average ± SD of triplicate samples. Results are representative of three independent experiments.

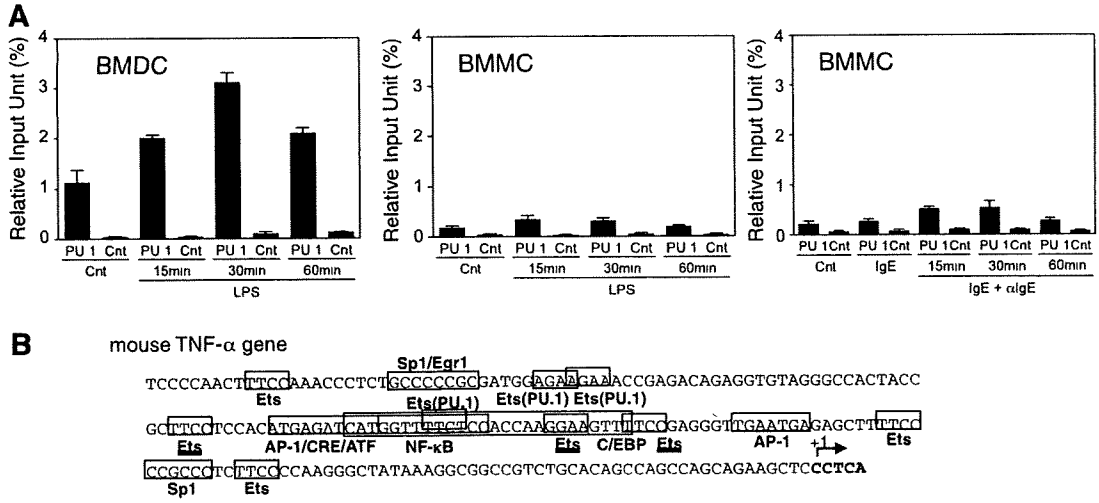

Fig. 2. PU.1 recruitments to the TNF-α promoter. (A) The amount of PU.1 binding to the TNF-α promoter in stimulated BMDC and BMMC. Data represent mean ± SD of PCR performed three times with duplicate samples for each ChIP. Similar results were obtained in two additional ChIP experiments. PU.1, anti-PU.1 Ab; Cnt, control Ab. (B) Nucleotide sequence of the mouse TNF-α promoter. *Cis*-enhancing elements identified in the human TNF-α promoter and conserved in the mouse TNF-α promoter are shown [16–18]. Ets boxes marked with underlined "Ets" were identified to be *cis*-enhancing elements in those studies. Additional consensus Ets-family protein binding sequences (GGAA) and PU.1-bindable sequences (AGAA) are boxed and marked with Ets and Ets (PU.1), respectively [8].

hypothesis, a ChIP assay was performed using retrovirus-transfected MC. The prepared BMMC with overexpression of PU.1 exhibited a high level of TNF-α production in response to LPS stimulation, equivalent to that of BMDC, while retaining weak expression of TLR4 (data not shown), as seen in our previous studies [12,13]. The relative input unit of PU.1 in the mock transfectants was moderately increased to approximately 0.5% by LPS stimulation (Fig. 3), which is consistent with the data of normal BMMC (Fig. 2A, middle). The occupancy of the TNF-α promoter by PU.1 in BMMC was significantly increased by transfection of PU.1-expressing retrovirus, and a further increase was observed following LPS-stimulation (Fig. 3). These results suggest that higher occupancy of the TNF-α promoter with PU.1 is one of the mechanisms that caused the higher production of TNF-α in the PU.1 transfectants.

Effect of PU.1 knockdown by siRNA on TNF-α and IL-6 production from stimulated BMDC

The results above demonstrate binding of PU.1 to the TNF-α promoter and an association between the amount of PU.1 on the promoter and the TNF-α expression level in stimulated BMDC and BMMC. Based on these observations, we performed PU.1 knockdown by siRNA to evaluate the effect of PU.1 in the expression of TNF-α. Introduction of PU.1 siRNA maintained the reduc-

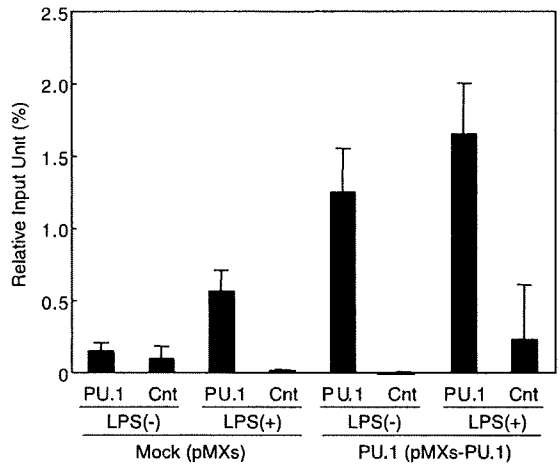

Fig. 3. Occupancy of PU.1 on the TNF-α promoter in PU.1-overexpressing cells. ChIP assays were performed using retrovirus transfectants carrying mock or PU.1 cDNA. Data represent mean ± SD of three PCRs with duplicate samples. Similar results were obtained in two additional ChIP experiments. PU.1, anti-PU.1 Ab; Cnt, control Ab.

tion of PU.1 mRNA levels at 5% of the control siRNA-introduced BMDC levels 24–48 h after electroporation (**Fig. 4**A). At 24 h post-siRNA treatment, the concentration of TNF-α protein in the culture medium of BMDC was determined at various time points following LPS-stimulation. As shown in **Fig. 4**B, the amount of TNF-α protein produced from PU.1 siRNA-introduced BMDC was markedly lower at 3 and 6 h. Such suppression was not observed in the concentration of IL-6 released from LPS-stimulated BMDC (**Fig. 4**C). This observation suggests that PU.1 is involved in the production of TNF-α in BMDC.

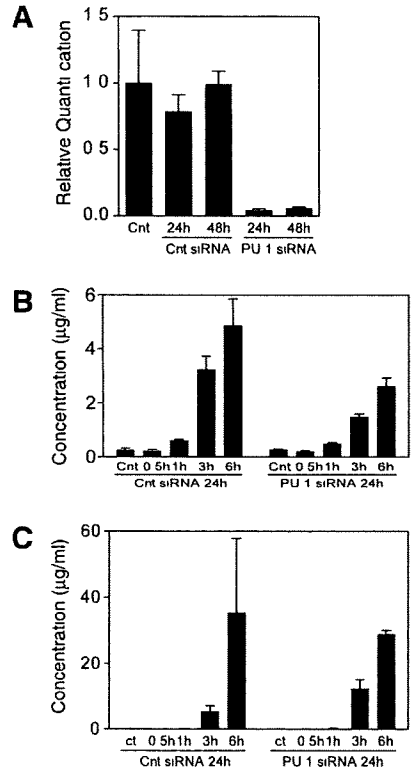

Fig. 4. Effect of PU.1 knockdown on the production of TNF-α from BMDC. The amount of PU.1 mRNA in siRNA-treated BMDC (A). Data represent mean ± SD of triplicate samples. Results are representative of three independent experiments. The concentration of TNF-α (B) and IL-6 (C) in culture medium of siRNA-treated BMDC. Data represent mean ± SD of two independent experiments with triplicate samples. Similar results of suppressed protein production were observed in another experiment.

Discussion

Several Ets-related motifs are present in the mouse TNF-α promoter, as shown in **Fig. 2**B. Three of them (labeled with underlined "Ets" in **Fig. 2**B) have been previously identified as *cis*-enhancing elements in LPS-stimulated activation of the TNF-α promoter in a human macrophage cell line [16,17]. The veracity of *in vitro* binding of PU.1 to these elements is controversial. In brief, the underlined Ets motif located at the most upstream region was reported to be bound to PU.1 in an EMSA experiment, but without provision of data [17]; however, PU.1 did not bind to this site in a DNaseI footprinting experiment even when binding of other Ets-family proteins, Ets-1 and Elk-1, was possible [16]. This Ets motif was also required for cytomegalovirus-mediated activation of the TNF-α promoter in monocytes and PU.1 was suggested to be a candidate transcription factor recognizing this element, although the binding of PU.1 against this sequence was not confirmed [19]. In the present study, we demonstrated the binding of PU.1 on the TNF-α promoter region of chromosome DNA in primary living DC by the ChIP assay and the involvement of PU.1 in TNF-α production by siRNA.

Introduction of PU.1 siRNA suppressed TNF-α production from LPS-stimulated BMDC. We cannot completely dismiss the possibility that PU.1 siRNA also down-regulated the expression and/or function of TLR4-signaling pathway-related molecules, although this pathway was not previously identified to be affected by PU.1 overexpression in MC [13]. However, we believe that PU.1 functions as a transactivator of the TNF-α promoter, based on the effect of PU.1 siRNA on TNF-α production and the lack of effect of PU.1 siRNA on the IL-6 promoter. In addition, IgE-mediated TNF-α production was also up-regulated, even under the conditions of IgE-signaling suppression, which cause a reduction in several IgE-mediated responses [13]. The TNF-α promoter in the PU.1-overexpressing cells was further occupied by PU.1 in the ChIP assay with retrovirus transfectants, also suggesting that TNF-α is the direct target of PU.1.

Previously, we found that PU.1-overexpressing MCs acquired high capacity for LPS-induced production of TNF-α and IL-6 to a similar degree [13], whereas in the present study PU.1 siRNA suppressed TNF-α expression but did not affect IL-6 expression in LPS-stimulated DCs. This discrepancy suggests that PU.1 acts both directly and indirectly in LPS-induced stimulation. PU.1 is directly involved in TNF-α transcription via direct interaction with the promoter in a TNF-α promoter-specific manner. The indirect effect of PU.1 may manifest as follows: an as yet unidentified molecule, which positively regulates LPS-induced stimulation signaling for expression of TNF-α and IL-6 in a similar manner, may be up-regulated by PU.1 in MCs but may not be down-regulated by PU.1 siRNA in DCs. Further studies to clarify the exact mechanism of the indirect effect of PU.1 are required to address this discrepancy in the results.

In the present study, the amount of PU.1 binding to the TNF-α promoter was increased following LPS-stimulation. LPS is known to activate PU.1 function by modulating the phosphorylation state of Ser in macrophages [27], which may one of the mechanisms of the rapid recruitment of PU.1 toward the promoter. In addition, LPS up-regulates the PU.1 protein levels in monocytes [27] and MCs [12]. Therefore, PU.1 involvement in LPS-induced transactivation of the TNF-α promoter may be mediated through at least two pathways.

DC introduced with PU.1 siRNA still possessed TNF-α producing capacity, although production was reduced. This remaining capacity may mean that the contribution of PU.1 to TNF-α promoter function is not as high as that of other transcription factors. Previously, several transcription factors, including the AP-1 family, Sp1, NF-kB, Egr-1, NF-ATp, Ets-1, and Elk-1, have been identified as binding to the TNF-α promoter [16,18]. To evaluate the degree of contribution of each transcription factor, the TNF-α production level should be compared among cells in the presence of each siRNA. Monocytes, macrophages, DC, T- and B-cells, MC, and fibroblasts are known to produce TNF-α. The expression of PU.1 is restricted in some of the myeloid- and lymphoid-lineages, and is detected in monocytes/macrophages/DC-lineage, the T/B-lineages, and MC, which is consistent with the TNF-α production profile. This observation may support the possible involvement of PU.1 in TNF-α promoter function. Considering the absence of PU.1 in fibroblasts, the effects of PU.1 on TNF-α promoter function may be restricted in TNF-α producing-hematopoietic cells, and this promoter may be regulated by a different combination of transcription factors in fibroblasts.

Acknowledgments

We are grateful to members of Atopy Research Center, Department of Immunology, and Department of Dermatology for helpful discussions. We thank Drs. Atsushi Takagi, Yusuke Niwa, Naomi Shimokawa, Qing-hui Wang, Nao Kitamura, and Mr. Hokuto Yokoyama for critical advice and support in experiments, and Ms. Michiyo Matsumoto for secretarial assistance. This study was supported in part by a Grant-in-aid for Scientific Research (C) (C.N.) from the Ministry of Education, Culture, Sports, Science, and Technology of Japan.

References

[1] J. Lloberas, C. Soler, A. Celara, The key role of PU.1/SPI-1 in B cells, myeloid cells and macrophages, Immunol. Today 20 (1999) 184–189.
[2] E.W. Scott, M.C. Simon, J. Anastasi, H. Singh, Requirement of transcription factor PU.1 in the development of multiple hematopoietic lineages, Science 265 (1994) 1573–1577.
[3] S.R. McKercher, B.E. Torbett, K.L. Anderson, G.W. Henkel, D.J. Vestal, H. Baribault, M. Klemsz, A.J. Feeney, G.E. Wu, C.J. Paige, R.A. Maki, Targeted disruption of the PU.1 gene results in multiple hematopoietic abnormalities, EMBO J. 15 (1996) 5647–5648.
[4] E.W. Scott, R.C. Fisher, M.C. Olson, E.W. Kehrli, M.C. Simon, H. Singh, PU.1 functions in a cell-autonomous manner to control the differentiation of multipotential lymphoid-myeloid progenitors, Immunity 6 (1997) 437–447.
[5] A. Guerriero, P.B. Langmuir, L.M. Spain, E.W. Scott, PU.1 is required for myeloid-derived but not lymphoid-derived dendritic cells, Blood 95 (2000) 879–885.
[6] K.L. Anderson, H. Perkin, C.D. Surh, S. Venturini, R.A. Maki, B.E. Torbett, Transcription factor PU.1 is necessary for development of thymic and myeloid progenitor-derived dendritic cells, J. Immunol. 164 (2000) 1855–1861.
[7] J.C. Walsh, R.P. DeKoter, H.-J. Lee, E.D. Smith, D.W. Lancki, M.F. Gurish, D.S. Friend, R.L. Stevens, J. Anastasi, H. Singh, Cooperative and antagonistic interplay between PU.1 and GATA-2 in the specification of myeloid cell fates, Immunity 17 (2002) 665–676.
[8] C. Nishiyama, M. Hasegawa, M. Nishiyama, K. Takahashi, Y. Akizawa, T. Yokota, K. Okumura, H. Ogawa, C. Ra, Regulation of human FcepsilonRI alpha-chain gene expression by multiple transcription factors, J. Immunol. 168 (2002) 4546–4552
[9] D.L. Galson, J.O. Hensold, T.R. Bishop, M. Shalling, A.D. D'andrea, C. Jones, P.E. Auron, D.E. Housman, Mouse beta-globin DNA-binding protein B1 is identical to a proto-oncogene, the transcription factor *Spi-1*/PU.1, and is restricted in expression to hematopoietic cells and testis, Mol. Cell. Biol. 13 (1993) 2929–2941.
[10] C. Nishiyama, M. Nishiyama, T. Ito, S. Masaki, K. Maeda, N. Masuoka, H. Yamane, T. Kitamura, H. Ogawa, K. Okumura, Overproduction of PU.1 in mast cell progenitors: its effect on monocyte- and mast cell-specific gene expression, Biochem. Biophys. Res. Commun. 313 (2004) 516–521
[11] C. Nishiyama, M. Nishiyama, T. Ito, S. Masaki, N. Masuoka, H. Yamane, T. Kitamura, H. Ogawa, K. Okumura, Functional analysis of PU.1 domains in monocyte-specific gene regulation, FEBS Lett. 561 (2004) 63–68.
[12] T. Ito, C. Nishiyama, M. Nishiyama, H. Matsuda, K. Maeda, Y. Akizawa, R. Tsuboi, K. Okumura, H. Ogawa, Mast cells acquire monocyte-specific gene expression and monocyte-like morphology by overproduction of PU.1, J. Immunol. 174 (2005) 376–383.
[13] Y. Niwa, C. Nishiyama, N. Nakano, A. Kamei, H. Kato, S. Kanada, S. Ikeda, H. Ogawa, K. Okumura, Opposite effects of PU.1 on mast cell stimulation, Biochem. Biophys. Res. Commun. 375 (2008) 95–100.
[14] M. Rehli, A. Poltorak, L. Schwarzfischer, S.W. Krause, R. Andreesen, B. Beutler, PU.1 and interferon consensus sequence-binding protein regulate the myeloid expression of the human Toll-like receptor 4 gene, J. Biol. Chem. 275 (2000) 9773–9781.
[15] M. Lichtinger, R. Ingram, M. Hornef, C. Bonifer, M. Rehli, Transcription factor PU.1 controls transcription start site positioning and alternative TLR4 promoter usage, J. Biol. Chem. 282 (2007) 26874–26883.
[16] E.Y. Tsai, J.V. Falvo, A.V. Tsytsykova, A.K. Barczak, A.M. Reimold, L.H. Glimcher, M.J. Fenton, D.C. Gordon, I.F. Dunn, A.E. Goldfeld, A. Lipopolysaccharide-specific enhancer complex involving Ets, Elk-1, Sp1, and CREB binding protein and p300 is recruited to the Tumor Necrosis Factor alpha promoter in vivo, Mol. Cell. Biol. 20 (2000) 6084–6094.
[17] J.H. Steer, K.M. Kroeger, L.J. Abraham, D.A. Joyce, Glucocorticoids suppress Tumor Necrosis Factor-alpha expression by human monocytic THP-1 cells by suppressing transactivation through adjacent NF-kappaB and c-Jun-activating transcription factor-2 binding sites in the promoter, J. Biol. Chem. 275 (2000) 18432–18440.
[18] B. Kramer, K. Wiegmann, M. Krönke, Regulation of the human TNF promoter by the transcription factor Ets, J. Biol. Chem. 270 (1995) 6577–6583.
[19] L.J. Geist, H.A. Hopkins, L.Y. Dai, B. He, M.M. Monick, G.W. Hunninghake, Cytomegalovirus modulates transcription factors necessary for the activation of the tumor necrosis factor-alpha promoter, Am. J. Respir. Cell Med. Biol. 16 (1997) 31–37.
[20] T. Nakahata, S.S. Spicer, J.R. Cantey, M. Ogawa, Clonal assay of mouse mast cell colonies in methylcellulose culture, Blood 60 (1982) 352–361.
[21] M.B. Lutz, N. Kukutsch, A.L.J. Ogilvie, S. Rößner, F. Koch, N. Romani, G. Schuler, An advanced culture method for generating large quantities of highly pure dendritic cells from mouse bone marrow, J. Immunol. Meth. 223 (1999) 77–92.
[22] N. Nakano, C. Nishiyama, S. Kanada, Y. Niwa, N. Shimokawa, H. Ushio, M. Nishiyama, K. Okumura, H. Ogawa, Involvement of mast cells in IL-12/23p40 production is essential for survival from polymicrobial infections, Blood 109 (2007) 4846–4855.
[23] C. Nishiyama, Y. Akizawa, M. Nishiyama, T. Tokura, H. Kawada, K. Mitsuishi, M. Hasegawa, T. Ito, N. Nakano, A. Okamoto, A. Takagi, H. Yagita, K. Okumura, H. Ogawa, Polymorphisms in the *FcepsilonRIbeta* promoter region affecting transcription activity: a possible promoter-dependent mechanism for association between *FcepsilonRIbeta* and atopy, J. Immunol. 173 (2004) 6458–6464.
[24] K. Maeda, C. Nishiyama, T. Tokura, H. Nakano, S. Kanada, M. Nishiyama, K. Okumura, H. Ogawa, FOG-1 represses GATA-1-dependent FcepsilonRI beta-chain transcription: transcriptional mechanism of mast cell-specific gene expression in mice, Blood 108 (2006) 262–269.
[25] S. Kanada, N. Nakano, D.P. Potaczek, K. Maeda, N. Shimokawa, Y. Niwa, T. Fukai, M. Sanak, A. Szczeklik, H. Yagita, K. Okumura, H. Ogawa, C. Nishiyama, Two different transcription factors discriminate the −315C>T polymorphism of the FcepsilonRIalpha gene: binding of Sp1 to −315C and of a high mobility group-related molecule to −315T, J. Immunol. 180 (2008) 8204–8210.
[26] Q.-H. Wang, C. Nishiyama, N. Nakano, N. Shimokawa, M. Hara, S. Kanada, H. Ogawa, K. Okumura, Suppressive effect of Elf-1 on FcepsilonRI alpha-chain expression in primary mast cells, Immunogenetics 60 (2008) 557–563.
[27] T.A. Lodie, R.S. Jr., D.T. Golenbock, C.P.V. Beveren, R.A. Maki, M.J. Fenton, Stimulation of macrophages by lipopolysaccharide alters the phosphorylation state, conformation, and function of PU.1 via activation of Casein Kinase II, J. Immunol. 158 (1997) 1848–1856.

ANTIMICROBIAL AGENTS AND CHEMOTHERAPY, May 2009, p. 1760–1765 Vol. 53, No. 5
0066-4804/09/$08.00+0 doi:10.1128/AAC.01540-08

Tetracyclines Modulate Protease-Activated Receptor 2-Mediated Proinflammatory Reactions in Epidermal Keratinocytes[▽]

Chika Ishikawa,† Tatsuya Tsuda,† Hiroe Konishi, Noboru Nakagawa, and Kiyofumi Yamanishi*

Department of Dermatology, Hyogo College of Medicine, Nishinomiya, Hyogo 663-8501, Japan

Received 19 November 2008/Returned for modification 17 December 2008/Accepted 16 February 2009

In addition to their antibiotic effects, tetracyclines have anti-inflammatory action that is often beneficial in the control of inflammatory skin disorders. In this study, we examined the effects of tetracycline (TET) and two of its derivatives, doxycycline (DOX) and minocycline (MIN), on the production of interleukin-8 (IL-8) elicited by the activation of protease-activated receptor 2 (PAR2) in normal human epidermal keratinocytes (NHEK). In NHEK, the production of IL-8 stimulated by an agonist peptide of PAR2, SLIGKIV-NH_2, at 100 μM was significantly reduced by TET, DOX, or MIN at 5 and 10 μM, concentrations that are noncytotoxic. The tumor necrosis factor alpha (TNF-α)-induced production of IL-8 was synergistically augmented by SLIGKIV-NH_2, and that synergistic increase in the production of IL-8 was suppressed by 100 nM *PAR2*-specific small interfering RNA. It was also suppressed by TET, DOX, or MIN but not by the 14-membered-ring macrolide antibiotics erythromycin, roxithromycin, and clarithromycin, which also have anti-inflammatory activities, at 10 μM. These results suggest that tetracyclines attenuate the PAR2–IL-8 axis in keratinocytes and thereby effectively modulate proinflammatory responses in the skin.

Tetracyclines are broad-spectrum antibiotics with a tetracyclic naphthacene carboxamide ring (18). In addition to their activities as antibiotics, tetracyclines show a variety of biological actions: anti-inflammatory activity, antiapoptosis activity, inhibition of proteolysis, and suppression of angiogenesis and tumor metastasis (21). Clinically, tetracyclines have been used to treat rheumatoid arthritis and various skin disorders, such as inflammatory acne, rosacea, bullous dermatoses, and neutrophilic dermatoses (12, 21). The anti-inflammatory activities of tetracyclines include the modulation of lymphocyte activation and neutrophil chemotaxis (6, 30), possibly by inhibiting matrix metalloproteinases (20), phospholipase A_2 (19), nitric oxide synthases (2), and/or caspase 1 (33). The ability of tetracyclines to bind Ca^{2+} and Mg^{2+} may account for some of those biological activities via the chelation of those cations and their transport into intracellular compartments (34). However, the exact molecular mechanism(s) of the immunomodulatory activities of tetracyclines in inflammatory skin disorders has not been fully delineated.

In response to various external stimuli and/or to endogenous proinflammatory cytokines, epidermal keratinocytes of the skin release chemokines such as interleukin-8 (IL-8), which recruit neutrophils and lymphocytes into the skin and exacerbate lesional inflammation (14). During inflammation of the skin, protease-activated receptor 2 (PAR2) (16) in keratinocytes is activated by serine proteases, such as leukocyte elastase (15) and mast cell tryptase (27), released from infiltrating immune cells. PAR2 activation amplifies the inflammation via the upregulation of intercellular cell adhesion molecule 1 (ICAM-1) expression (5) and the release of IL-8 from keratinocytes (Fig. 1). Thus, the activation of PAR2 and/or its signaling pathways in the epidermis plays a pivotal role in inflammatory processes and their amplification in the skin.

We have recently shown that 14-membered-ring macrolides, which have immunomodulatory activities, suppress the IL-1β-induced production of IL-8 that is synergized by the activation of PAR2, and we proposed the PAR2–IL-8 axis as a therapeutic target for the control of cutaneous inflammation (32). The aim of the present study was to determine whether tetracyclines, which have anti-inflammatory activities, also modulate the PAR2-mediated proinflammatory responses of keratinocytes.

MATERIALS AND METHODS

Materials. SLIGKV-NH_2 and its reverse peptide, VKGILS-NH_2, were from Bachem Inc (Torrance, CA) and Sigma-Aldrich Corp. (St Louis, MO), respectively. IL-1β, tumor necrosis factor alpha (TNF-α), and gamma interferon (IFN-γ) were from Peprotech EC Ltd. (London, United Kingdom). Tetracycline HCl was purchased from Nacalai Tesque, Inc (Kyoto, Japan), and minocycline HCl and doxycycline HCl were from Sigma-Aldrich Corp.

Cell culture. Normal human epidermal keratinocytes (NHEK) (Cambrex BioScience Inc., Baltimore, MD) were seeded into T75 flasks (Corning Inc./Life Sciences, Acton, MA) at a density of 2×10^5 cells per flask in 10 ml KGM2 medium (Kurabo Industries Ltd., Osaka, Japan). The cells were incubated at 37°C under an atmosphere of 5% CO_2 in 95% air. When the cells became 75% confluent, they were trypsinized and subcultured into 12-well plates at an initial seeding density of 1×10^4 cells per cm^2.

Transient transfection and knockdown of PAR2. NHEK seeded into 12-well plates were incubated for 72 h, after which they were transfected with a *PAR2*-specific small interfering RNA (siRNA) (Qiagen, Inc., Hilden, Germany) by using the TransIT TKO transfection reagent (Mirus Bio Corp., Madison, WI) according to the manufacturer's instructions. After 24 h of incubation, the cells were treated with a cytokine and/or an agonist peptide, and 24 h later, the cells were harvested for RNA isolation.

qRT-PCR. Total RNAs were isolated from NHEK using the TRI reagent (Sigma-Aldrich Corp.), and cDNAs were synthesized using TaqMan reverse transcription reagents (Applied Biosystems, Foster City, CA). An ABI 7900HT sequence detection system (Applied Biosystems) was used for quantitative real-time PCR (qRT-PCR). An mRNA encoding glyceraldehyde-3-phosphate dehydrogenase (GAPDH) was used as an internal standard for qRT-PCR. The product numbers of the primers and probes for PAR2 and GAPDH, which were

* Corresponding author. Mailing address: Department of Dermatology, Hyogo College of Medicine, Nishinomiya, Hyogo 663-8501, Japan. Phone: 81-798-45-6653. Fax: 81-798-45-6651. E-mail: kyamanis@hyo-med.ac.jp.

† C.I. and T.T. contributed equally to this work.

▽ Published ahead of print on 2 March 2009.

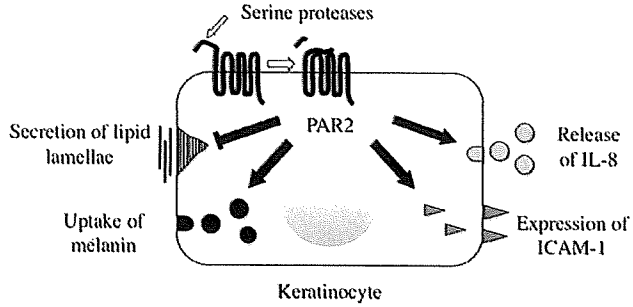

FIG. 1. Activation and function of PAR2 in keratinocytes. Serine proteases cleave the N-terminal arm of PAR2, and the exposed new N-terminal peptide can activate the receptor. The activation of PAR2 accelerates the release of IL-8 from the cells and increases the expression of ICAM-1 and the uptake of melanin from melanocytes but suppresses the secretion of lipid lamellae, which is essential for skin barrier homeostasis.

obtained from Applied Biosystems Assays-on-Demand, are Hs 00608346 m1 and Hs 99999905 m1, respectively. The relative abundance of each target transcript was assessed with regard to internal controls according to the manufacturer's instructions. Experiments were repeated at least three times, and results are expressed as mean levels of induction of PAR2 transcripts ± standard deviations (n = 3).

ELISA for IL-8. NHEK seeded into 12-well plates were incubated for 72 h, and the medium was changed to KGM2 without additives. Cells were preincubated for 24 h in the presence or absence of each antibiotic, after which the agonist peptide SLIGKV-NH_2 or its reverse peptide, VKGILS-NH_2, and/or IL-1β (100 ng/ml) or TNF-α (100 ng/ml) was added. Forty-eight hours later, culture media were collected and assayed for IL-8 by using a Quantikine human IL-8 enzyme-linked immunosorbent assay (ELISA) kit (R&D Systems, Inc., Minneapolis, MN). Experiments were repeated at least three times, and results are expressed as means ± standard deviations for triplicate samples.

Cell viability assay. Cell viability was assessed using a modified 3-(4,5-dimethyl-2-thiazolyl)-2,5-diphenyl-2H-tetrazolium bromide (MTT) assay kit (Cell Counting kit 8; Dojindo Molecular Technologies, Inc., Gaithersburg, MD), according to the manufacturer's instructions. NHEK seeded into 24-well plates were incubated for 72 h, and the medium was changed to KGM2 without additives. The cells were then preincubated for 24 h in the presence or absence of each antibiotic. Forty-eight hours later, the kit reagent WST-8 was added directly to the culture medium, and the culture was incubated for an additional 1 h, after which the absorbance of formazan was measured at 450 nm by spectrophotometry.

Statistical analysis of data. Data are expressed as means ± standard deviations. One-way analysis of variance followed by Scheffe's test or Student's two-tailed t test was performed for statistical analysis of data. A P value of < 0.05 was considered statistically significant.

RESULTS

Effects of tetracyclines on IL-8 production stimulated by the PAR2 agonist peptide. Proteolytic cleavage of PAR2 by serine proteases exposes a new NH_2 terminus domain that serves as a tethered ligand for the receptor itself (16) (Fig. 1). A synthetic receptor-activating peptide, SLIGKV-NH_2, which has a sequence identical to that of the human PAR2-tethered ligand domain, mimics the actions of the serine proteases (9). When NHEK were treated with 100 μM SLIGKV-NH_2 for 48 h, the concentration of IL-8 in the medium increased (Fig. 2). Prior to examination of the effects of tetracycline (TET), doxycycline (DOX), or minocycline (MIN) on the PAR2-mediated production of IL-8, the possible cytotoxic effects of these drugs on NHEK were assessed using a modified MTT assay. NHEK were treated with TET, DOX, or MIN for 72 h, after which the formazan absorbance in the culture medium was measured. Cell viability was drastically decreased at 100 μM TET, DOX, or MIN but not at concentrations of 10 μM or lower (data not shown). Therefore, we used 10 μM and lower concentrations of these tetracyclines for further experiments.

The effects of tetracyclines on the PAR2-mediated stimulation of IL-8 production were assessed in NHEK that had been preincubated with TET, DOX, or MIN for 24 h prior to the addition of 100 μM SLIGKV-NH_2. TET at a concentration of 5 or 10 μM slightly but significantly decreased the concentration of IL-8 in the medium of SLIGKV-NH_2-treated NHEK (Fig. 2A). DOX also significantly decreased the IL-8 levels at these concentrations (Fig. 2B). MIN at a concentration of 5 or 10 μM reduced the SLIGKV-NH_2-induced increase in the level of IL-8 (Fig. 2C). When each tetracycline was added simultaneously with SLIGKV-NH_2, the effect was similar to, or a little less than, that in cells treated 24 h before the addition of the agonist peptide. When these drugs were added after the addition of SLIGKV-NH_2, none of them affected the production of IL-8 (data not shown).

Because the production of IL-8 stimulated by PAR2 activation is dependent on PAR2 gene expression (32), these tetracyclines might decrease the expression of the PAR2 gene. This possibility was assessed by qRT-PCR, but when NHEK were treated with 10 μM TET, DOX, or MIN for 48 h, the expression of the PAR2 gene was not reduced (Fig. 2D).

Effect of the PAR2 agonist peptide on the TNF-α- or IFN-γ-induced production of IL-8. We examined whether the activation of PAR2 affects the IL-8-inducing capability of the proinflammatory cytokines TNF-α and IFN-γ. When NHEK were treated with 100 ng/ml TNF-α or 100 μM SLIGKV-NH_2 for 48 h, the concentration of IL-8 in the medium increased (Fig. 3A). Moreover, combined treatment with 100 ng/ml TNF-α and 100 μM SLIGKV-NH_2 caused a synergistic increase in IL-8 levels that was greater than the sum of the separate effects of TNF-α and SLIGKV-NH_2 at the same doses. However, in NHEK transfected with 100 nM *PAR2*-specific siRNA, the basal level of IL-8 decreased and, regardless of the presence or absence of SLIGKV-NH_2, the effect of TNF-α was significantly suppressed. When the reverse control peptide VKGILS-NH_2 was used in place of SLIGKV-NH_2, IL-8 production by NHEK was not increased. Furthermore, VKGILS-NH_2 induced no synergistic increase in IL-8 levels, even in the presence of 100 ng/ml TNF-α (data not shown).

When NHEK were treated with 100 ng/ml IFN-γ, IL-8 levels increased and were similar to levels in NHEK treated with 100 μM SLIGKV-NH_2 (Fig. 3B). In the presence of both IFN-γ and SLIGKV-NH_2, IL-8 levels were increased, but no synergistic increase was observed. IFN-γ-induced increases in IL-8 levels were significantly reduced in NHEK transfected with the *PAR2*-specific siRNA.

Effects of tetracyclines on the synergistic stimulation of IL-8 production induced by IL-1β or TNF-α with the PAR2 agonist peptide. We then assessed whether tetracyclines modulate the PAR2-mediated synergistic increase in IL-8 production by NHEK. TET, DOX, or MIN (at a concentration of 10 μM) was added to NHEK 24 h before treatment with 100 μM SLIGKV-NH_2 and/or 100 ng/ml IL-1β or TNF-α. In NHEK treated with IL-1β, 10 μM TET did not show any significant effect on the concentration of IL-8 in the medium, even in the presence of

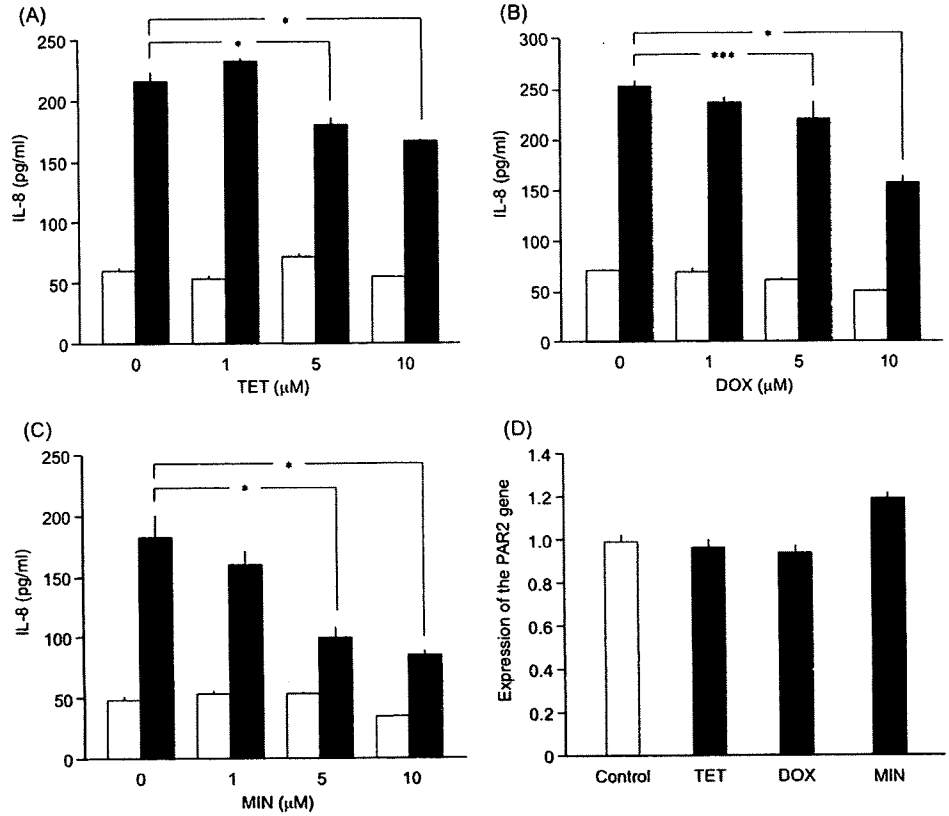

FIG. 2. Effects of tetracyclines on the SLIGKV-NH_2-induced production of IL-8 by NHEK and on the expression of the *PAR2* gene. (A to C) In the presence or absence of the indicated concentration of TET (A), DOX (B), or MIN (C), NHEK were treated with 100 μM SLIGKV-NH_2 for 48 h, after which the concentration of IL-8 in the culture medium was measured by ELISA. Open bars, control; filled bars, SLIGKV-NH_2-treated cells. Analysis of variance followed by Scheffe's test was performed for statistical analysis of data. *, $P < 0.001$; ***, $P < 0.05$. (D) Effect of TET, DOX, or MIN on the expression of the *PAR2* gene in NHEK. NHEK were incubated without any drug (open bars) or with 10 μM TET, DOX, or MIN (filled bars) for 48 h, and the levels of PAR2 transcripts were determined by qRT-PCR.

SLIGKV-NH_2 (Fig. 4A). In NHEK treated with TNF-α, the synergistic increase in IL-8 production elicited by SLIGKV-NH_2 was slightly but significantly suppressed by treatment with TET (Fig. 4A). DOX also significantly decreased the agonist peptide-stimulated production of IL-8 in IL-1β- or TNF-α-treated NHEK (Fig. 4B). MIN substantially reduced the synergistic increases in IL-8 levels, although the reduced levels were not as low as those in control cells treated with SLIGKV-NH_2 (data not shown), IL-1β, or TNF-α alone (Fig. 4C).

Effects of 14-membered-ring macrolides on the synergistic stimulation of IL-8 production by TNF-α and the PAR2 agonist peptide. The 14-membered-ring macrolides erythromycin (ERY), roxithromycin (RXM), and clarithromycin (CLR) attenuate the IL-1β-induced production of IL-8 in NHEK, which can be synergized by treatment with SLIGKV-NH_2 (32). Hence, we examined whether these macrolides would affect the production of IL-8 induced by the PAR2 agonist peptide and TNF-α. However, in contrast to the effects of these macrolides on IL-1β-treated NHEK, treatment with 10 μM ERY (Fig. 5A), RXM (Fig. 5B), or CLR (Fig. 5C) did not decrease the concentration of IL-8 in the medium of NHEK treated with both 100 μM SLIGKV-NH_2 and 100 ng/ml TNF-α.

DISCUSSION

PAR2 is a member of the unique G-protein-coupled receptor subfamily with seven transmembrane domains and is expressed abundantly in various organs, including the skin. Recent findings suggest that PAR2 is involved in various aspects of skin pathophysiology (Fig. 1), including melanin transfer (23), itch generation due to mast cell tryptase (27), and epidermal barrier homeostasis via the suppressed secretion of lipid lamellae from keratinocytes (8). PAR2 binding to G proteins has been shown in the epidermis, especially in the stratum granulosum (26) and in skin affected by the inflammatory process. The suppression of allergic and toxic contact dermatitis in PAR2 knockout mice suggests an important role for PAR2 in cutaneous inflammation (22). We have focused on the proinflammatory role of PAR2 in keratinocytes as a novel target for the treatment of cutaneous inflammation.

Tetracyclines are useful as options for treating a variety of inflammatory skin disorders and can be administered orally (21). In the present study, we show a novel biological activity of TET and two of its derivatives, MIN and DOX, that attenuates the PAR2-mediated production of IL-8 by keratinocytes. These tetracyclines decrease the production of IL-8 at concen-

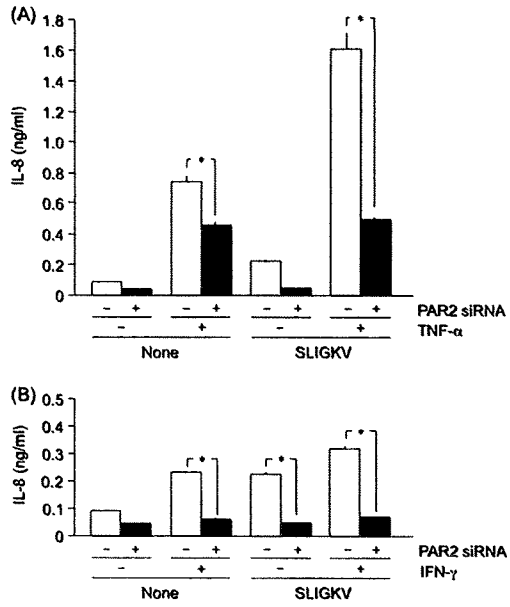

FIG. 3. Effects of SLIGKV-NH_2 and a *PAR2*-specific siRNA on TNF-α- or IFN-γ-induced production of IL-8 by NHEK. NHEK were transfected with 100 nM *PAR2*-specific siRNA for 24 h as indicated and were then treated with 100 ng/ml TNF-α (A) or IFN-γ (B) with or without 100 μM SLIGKV-NH_2. After 24 h of incubation, the concentration of IL-8 in the culture medium was measured by ELISA. Student's two-tailed *t* test was performed for statistical analysis of data. *, $P < 0.001$. Open bars, control; filled bars, cells transfected with the *PAR2*-specific siRNA.

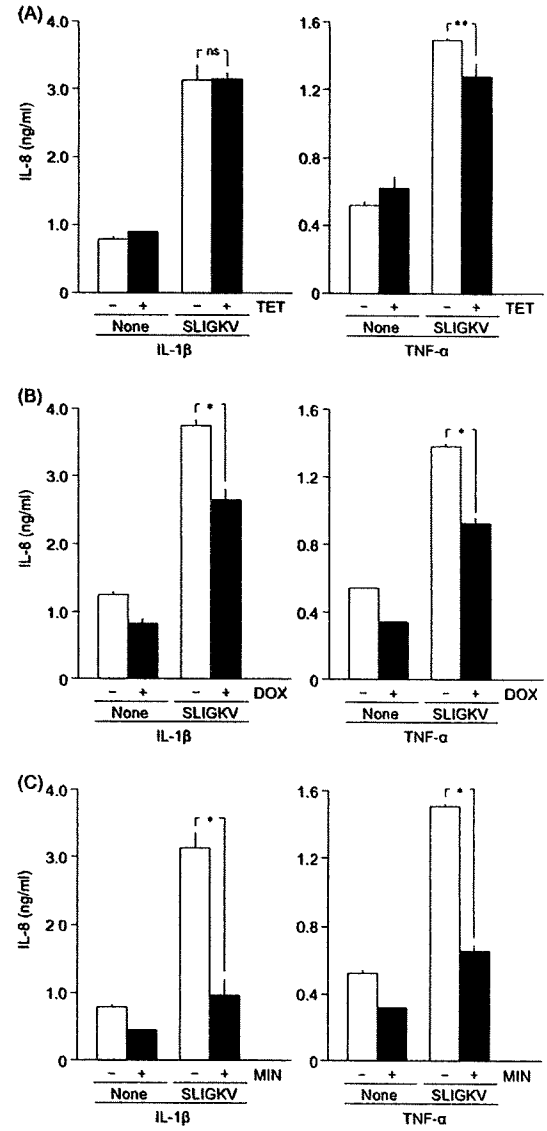

FIG. 4. Effects of tetracyclines on the synergistic production of IL-8 induced by SLIGKV-NH_2 in IL-1β- or TNF-α-treated NHEK. In the presence or absence of 10 μM TET (A), DOX (B), or MIN (C), NHEK were treated with 100 ng/ml IL-1β or TNF-α and/or 100 μM SLIGKV-NH_2 for 48 h. The concentration of IL-8 in the culture medium was then measured by ELISA. Open bars, control; filled bars, cells treated with TET, DOX, or MIN. Student's two-tailed *t* test was performed for statistical analysis of data. *, $P < 0.001$; **, $P < 0.01$; ns, not significant.

trations of 10 μM (Fig. 2A to C), which approach the therapeutic concentrations of those drugs in serum (1) and are not cytotoxic to keratinocytes in culture. The PAR2-mediated production of IL-8 depends on the expression of the *PAR2* gene (32), which is not reduced by the concentrations of tetracyclines used (Fig. 2D). Therefore, it is unlikely that the effects of these tetracyclines on the production of IL-8 are due to decreased expression of the PAR2 gene.

Proinflammatory cytokines, matrix metalloproteinases, and antimicrobial peptides are upregulated in the inflammatory stage of acne (31), which can be effectively treated with tetracyclines. One reason for the favorable effects of tetracyclines on cutaneous inflammation may be a reduction of neutrophil chemotaxis (6, 7). The present study suggests that the therapeutic effects of tetracyclines may be due, at least in part, to modulation of the PAR2-mediated production of IL-8, which recruits neutrophils to the inflammatory lesions. Tetracyclines are also effective for the treatment of rosacea (24). In skin with rosacea, PAR2 is widely expressed by keratinocytes, in which endogenous proteases such as kallikrein-related peptidases that activate PAR2 are upregulated (25). Therefore, the effectiveness of tetracyclines for treating rosacea might also be PAR2 mediated, although alternative mechanisms involving angiogenesis have been postulated (21).

The proinflammatory cytokine IL-1 strongly induces the production of IL-8 by NHEK, and the effect of IL-1 is synergized by the stimulation of PAR2 (9, 10, 32). We show evidence that the activation of PAR2 markedly enhances the production of IL-8 induced by TNF-α as well as that induced by IL-1 in NHEK, whereas the stimulation of PAR2 does not potentiate the effect of IFN-γ (Fig. 3). Thus, the signals from PAR2 interact with those from some cytokines to amplify their responses. Such a booster effect has been observed in keratinocytes when TNF-α is administered in combination with IFN-γ (3, 29), but it is not clear whether PAR2 uses the same signaling system as IFN-γ for the induction of IL-8 in keratinocytes.

We show in this study that tetracyclines suppress the PAR2-mediated synergistic enhancement of IL-8 production induced

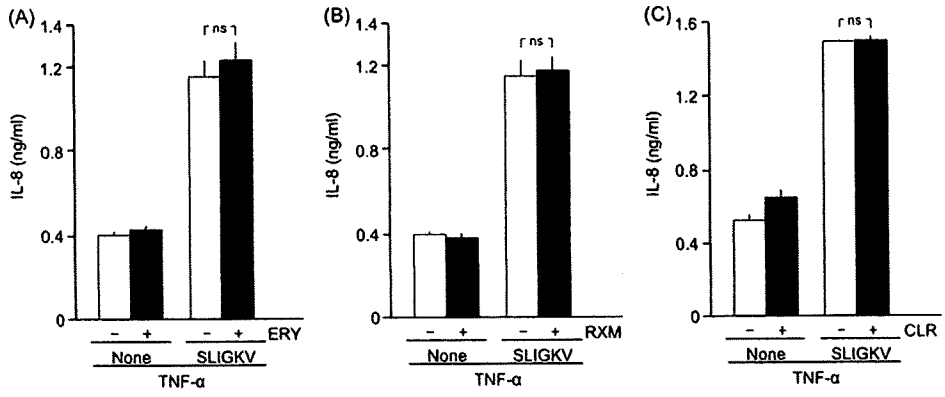

FIG. 5. Effects of the 14-membered-ring macrolides ERY, RXM, and CLR on the synergistic production of IL-8 induced by SLIGKV-NH_2 in TNF-α-treated NHEK. In the presence or absence of 10 μM ERY (A), RXM (B), or CLR (C), NHEK were treated with 100 ng/ml TNF-α and/or 100 μM SLIGKV-NH_2 for 48 h. The concentration of IL-8 in the culture medium was then measured by ELISA. Open bars, control; filled bars, cells treated with ERY, RXM, or CLR. Student's two-tailed *t* test was performed for statistical analysis of data. ns, not significant.

by IL-1 and TNF-α in NHEK (Fig. 4). The anti-inflammatory effects of tetracyclines on skin disorders might be due, at least in part, to suppression of the synergized production of IL-8 by keratinocytes. The effect of MIN is greater than that of DOX; in contrast, TET is less effective (Fig. 4). The different efficacies among tetracyclines have also been reported with regard to other biological processes, such as nitric oxide synthesis (2) and inactivation of glial cells (35). MIN and DOX are more lipophilic than TET, and the lipid solubility of MIN is almost twice that of DOX (4, 11). The different lipophilicities of these drugs might affect their passage across the plasma membrane into cells. The activation of PAR2 transiently increases intracellular Ca^{2+} levels in keratinocytes, which trigger the downstream binding of NF-κB to DNA (17, 25). The chelation of Ca^{2+} by MIN or DOX might suppress the downstream signal transduction for the enhanced production of IL-8 (18). The possibility that these tetracyclines bind SLIGKV-NH_2 or otherwise interfere with its binding to PAR2 has not been examined in the present study.

We have recently shown that 14-membered-ring macrolides, such as ERY and RXM, suppress the IL-1β-induced production of IL-8 synergized by the activation of PAR2 (32). Interestingly, however, these macrolides do not affect TNF-α-induced synergism, as shown in this study (Fig. 5). This suggests that these macrolides modulate the synergistic production of IL-8 in different ways from MIN and DOX. Komine et al. have shown that RXM suppresses p38 phosphorylation and NF-κB-driven transcription independently of the inhibition of IκB degradation in HaCaT cells, a keratinocyte cell line (13). Takahashi et al. (28) have also reported that RXM reduces the transcriptional activities of both AP-1 and NF-κB in NHEK. Whether MIN and DOX interfere with these particular signaling molecules and/or transcription factors in keratinocytes has not been determined, but common signaling systems might be affected by MIN and DOX and by these macrolides, at least in the PAR2-mediated synergistic production of IL-8 induced by IL-1β.

During the course of cutaneous inflammation, keratinocytes release abundant amounts of IL-8 in response to proinflammatory cytokines such as IL-1 and TNF-α, which are amplified by the activation of PAR2, possibly triggered by upregulated kallikrein-related peptidases from lesional keratinocytes (25) and/or by other serine proteases from infiltrating inflammatory cells. PAR2 in the epidermis plays a pivotal role as a sensor, the activation of which leads to the exacerbation of skin inflammation. Tetracycline derivatives exhibit a novel activity, distinct from their antibiotic effects, that modulates the PAR2–IL-8 axis and attenuates the proinflammatory process in epidermal keratinocytes. The modulatory effects of those tetracyclines might explain their effectiveness in treating various inflammatory skin disorders.

ACKNOWLEDGMENTS

We thank members of the Joint-Use Research Facilities of the Hyogo College of Medicine for technical assistance.

This work was partially supported by the Ministry of Education, Science, Sports and Culture through a Grant-in-Aid for Scientific Research and for Young Scientists; by a High-Tech Research Center Grant; by a grant from the Ministry of Health, Labor and Welfare (Health and Labor Sciences Research Grants for Research on Intractable Diseases); and by a Grant-in-Aid for researchers, from the Hyogo College of Medicine.

REFERENCES

1. **Agwuh, K. N., and A. MacGowan.** 2006. Pharmacokinetics and pharmacodynamics of the tetracyclines including glycylcyclines J. Antimicrob Chemother **58**:256–265
2. **Amin, A. R., M. G. Attur, G. D. Thakker, P. D. Patel, P. R. Vyas, R. N. Patel, I. R. Patel, and S. B. Abramson.** 1996 A novel mechanism of action of tetracyclines. effects on nitric oxide synthases. Proc Natl. Acad. Sci USA **93**:14014–14019
3. **Barker, J. N., V. Sarma, R. S. Mitra, V. M. Dixit, and B. J. Nickoloff.** 1990. Marked synergism between tumor necrosis factor-α and interferon-γ in regulation of keratinocyte-derived adhesion molecules and chemotactic factors J. Clin. Investig **85**:605–608.
4. **Barza, M., R. B. Brown, C. Shanks, C. Gamble, and L. Weinstein.** 1975 Relation between lipophilicity and pharmacological behavior of minocycline, doxycycline, tetracycline. and oxytetracycline in dogs. Antimicrob Agents Chemother **8**:713–720.
5. **Buddenkotte, J., C. Stroh, I. H. Engels, C. Moormann, V. M. Shpacovitch, S. Seeliger, N. Vergnolle, D. Vestweber, T. A. Luger, K. Schulze-Osthoff, and M. Steinhoff.** 2005. Agonists of proteinase-activated receptor-2 stimulate upregulation of intercellular cell adhesion molecule-1 in primary human keratinocytes via activation of NF-κB. J. Investig. Dermatol **124**:38–45
6. **Esterly, N. B., N. L. Furey, and L. E. Flanagan.** 1978. The effect of antimicrobial agents on leukocyte chemotaxis. J. Investig Dermatol. **70**:51–55
7. **Esterly, N. B., J. S. Koransky, N. L. Furey, and M. Trevisan.** 1984 Neutro-

phil chemotaxis in patients with acne receiving oral tetracycline therapy Arch Dermatol **120**:1308–1313.
8. **Hachem, J. P., E. Houben, D. Crumrine, M. Q. Man, N. Schurer, T. Roelandt, E. H. Choi, Y. Uchida, B. E. Brown, K. R. Feingold, and P. M. Elias.** 2006. Serine protease signaling of epidermal permeability barrier homeostasis J. Investig. Dermatol. **126**:2074–2086.
9. **Hou, L., S. Kapas, A. T. Cruchley, M. G. Macey, P. Harriott, C. Chinni, S. R. Stone, and G. L. Howells.** 1998. Immunolocalization of protease-activated receptor-2 in skin: receptor activation stimulates interleukin-8 secretion by keratinocytes in vitro Immunology **94**:356–362.
10. **Iwakiri, K., M. Ghazizadeh, E. Jin, M. Fujiwara, T. Takemura, S. Takezaki, S. Kawana, S. Yasuoka, and O. Kawanami.** 2004. Human airway trypsin-like protease induces PAR-2-mediated IL-8 release in psoriasis vulgaris. J. Investig Dermatol. **122**:937–944.
11. **Klein, N. C., and B. A. Cunha.** 1995. Tetracyclines. Med Clin. N Am. **79**:789–801.
12. **Kloppenburg, M., F. C. Breedveld, J. P. Terwiel, C. Mallee, and B. A. Dijkmans.** 1994. Minocycline in active rheumatoid arthritis. A double-blind, placebo-controlled trial. Arthritis Rheum. **37**:629–636
13. **Komine, M., T. Kakinuma, S. Kagami, Y. Hanakawa, K. Hashimoto, and K. Tamaki.** 2005. Mechanism of thymus- and activation-regulated chemokine (TARC)/CCL17 production and its modulation by roxithromycin. J. Investig Dermatol **125**:491–498.
14. **Larsen, C. G., A. O. Anderson, J. J. Oppenheim, and K. Matsushima.** 1989. Production of interleukin-8 by human dermal fibroblasts and keratinocytes in response to interleukin-1 or tumour necrosis factor. Immunology **68**:31–36.
15. **Ludolph-Hauser, D., C. Schubert, and O. Wiedow.** 1999. Structural changes of human epidermis induced by human leukocyte-derived proteases. Exp. Dermatol. **8**:46–52
16. **Macfarlane, S. R., M. J. Seatter, T. Kanke, G. D. Hunter, and R. Plevin.** 2001. Proteinase-activated receptors. Pharmacol. Rev. **53**:245–282.
17. **Macfarlane, S. R., C. M. Sloss, P. Cameron, T. Kanke, R. C. McKenzie, and R. Plevin.** 2005. The role of intracellular Ca^{2+} in the regulation of proteinase-activated receptor-2 mediated nuclear factor κB signalling in keratinocytes. Br. J. Pharmacol. **145**:535–544.
18. **Nelson, M. L.** 1998. Chemical and biological dynamics of tetracyclines. Adv. Dent. Res. **12**:5–11.
19. **Pruzanski, W., R. A. Greenwald, I. P. Street, F. Laliberte, E. Stefanski, and P. Vadas.** 1992 Inhibition of enzymatic activity of phospholipases A2 by minocycline and doxycycline Biochem. Pharmacol. **44**:1165–1170.
20. **Sadowski, T., and J. Steinmeyer.** 2001. Effects of tetracyclines on the production of matrix metalloproteinases and plasminogen activators as well as of their natural inhibitors, tissue inhibitor of metalloproteinases-1 and plasminogen activator inhibitor-1. Inflamm. Res. **50**:175–182.
21. **Sapadin, A. N., and R. Fleischmajer.** 2006. Tetracyclines: nonantibiotic properties and their clinical implications. J. Am. Acad. Dermatol. **54**:258–265.
22. **Seeliger, S., C. K. Derian, N. Vergnolle, N. W. Bunnett, R. Nawroth, M. Schmelz, P. Y. Von Der Weid, J. Buddenkotte, C. Sunderkotter, D. Metze, P. Andrade-Gordon, E. Harms, D. Vestweber, T. A. Luger, and M. Steinhoff.** 2003. Proinflammatory role of proteinase-activated receptor-2 in humans and mice during cutaneous inflammation in vivo. FASEB J **17**:1871–1885
23. **Seiberg, M., C. Paine, E. Sharlow, P. Andrade-Gordon, M. Costanzo, M. Eisinger, and S. S. Shapiro.** 2000. The protease-activated receptor 2 regulates pigmentation via keratinocyte-melanocyte interactions. Exp. Cell Res **254**:25–32
24. **Sneddon, I. B.** 1976. The treatment of steroid-induced rosacea and perioral dermatitis. Dermatologica **152**(Suppl 1):231–237
25. **Stefansson, K., M. Brattsand, D. Roosterman, C. Kempkes, G. Bocheva, M. Steinhoff, and T. Egelrud.** 2008. Activation of proteinase-activated receptor-2 by human kallikrein-related peptidases. J Investig Dermatol **128**:18–25
26. **Steinhoff, M., C. U. Corvera, M. S. Thoma, W. Kong, B. E. McAlpine, G. H. Caughey, J. C. Ansel, and N. W. Bunnett.** 1999 Proteinase-activated receptor-2 in human skin: tissue distribution and activation of keratinocytes by mast cell tryptase Exp. Dermatol. **8**:282–294
27. **Steinhoff, M., U. Neisius, A. Ikoma, M. Fartasch, G. Heyer, P. S. Skov, T. A. Luger, and M. Schmelz.** 2003. Proteinase-activated receptor-2 mediates itch: a novel pathway for pruritus in human skin. J Neurosci **23**:6176–6180
28. **Takahashi, H., Y. Hashimoto, A. Ishida-Yamamoto, and H. Iizuka.** 2005. Roxithromycin suppresses involucrin expression by modulation of activator protein-1 and nuclear factor-κB activities of keratinocytes. J. Dermatol Sci. **39**:175–182.
29. **Teunissen, M. B., C. W. Koomen, R. de Waal Malefyt, E. A. Wierenga, and J. D. Bos.** 1998 Interleukin-17 and interferon-γ synergize in the enhancement of proinflammatory cytokine production by human keratinocytes. J Investig Dermatol. **111**:645–649.
30. **Thong, Y. H., and A. Ferrante.** 1979. Inhibition of mitogen-induced human lymphocyte proliferative responses by tetracycline analogues. Clin. Exp. Immunol **35**:443–446.
31. **Trivedi, N. R., K. L. Gilliland, W. Zhao, W. Liu, and D. M. Thiboutot.** 2006. Gene array expression profiling in acne lesions reveals marked upregulation of genes involved in inflammation and matrix remodeling. J Investig. Dermatol. **126**:1071–1079.
32. **Tsuda, T., C. Ishikawa, H. Konishi, Y. Hayashi, N. Nakagawa, M. Matsuki, H. Mizutani, and K. Yamanishi.** 2008. Effect of 14-membered-ring macrolides on production of interleukin-8 mediated by protease-activated receptor 2 in human keratinocytes. Antimicrob. Agents Chemother. **52**:1538–1541
33. **Vincent, J. A., and S. Mohr.** 2007 Inhibition of caspase-1/interleukin-1β signaling prevents degeneration of retinal capillaries in diabetes and galactosemia. Diabetes **56**:224–230.
34. **White, J. R., and F. L. Pearce.** 1982. Characterization of chlortetracycline (aureomycin) as a calcium ionophore. Biochemistry **21**:6309–6312
35. **Yrjänheikki, J., R. Keinanen, M. Pellikka, T. Hokfelt, and J. Koistinaho.** 1998. Tetracyclines inhibit microglial activation and are neuroprotective in global brain ischemia. Proc. Natl. Acad. Sci USA **95**:15769–15774.

Acknowledgments

We are grateful to Dr. Takaaki Itou, Livestock Medical Center, Aichi Prefectural Federation of Agricultural Mutual Aid Association, for the kind gift of clinical isolates, and to Dr. Motofumi Suzuki, RIKEN BioResource Center, Wako, Saitama, Japan, for kindly providing the *Prototheca* reference strains. We thank Dr. Rui Kano for critical discussion, Dr. Takafumi Osumi for technical assistance with assimilation pattern testing, Department of Pathobiology, School of Veterinary Medicine, Nihon University, Fujisawa Kanagawa, Japan.

References

[1] Pore RS. *Prototheca*, a yeast-like alga. In: Kurtzman CP, Fell JW, editors. The Yeast, A Taxonomic Study. 4th edn, Amsterdam: Elsevier Science; 1998. p. 881–7.
[2] Cornelia Lass-Florl. Astrid mayr: human protothecosis. Clin Mycrobiol Rev 2007;20:230–42.
[3] Leimann BC, Monteiro PC, Lazéra, Lazera M, Candanoza ER. Wanke B Protothecosis Med Mycol 2004;42:95–106.
[4] Ikeda T. Ghoma M: protothecosis in animals. Vet Darmatol Japan 2002;8:23–32.
[5] Bueno VF, de Mesquita AJ, Neves RB, de Souza MA, Ribero AR, Nicolau ES, et al. Epidemiological and clinical aspects of the first outbreak of bovine mastitis caused by *Prototheca zopfii* in Goiás State, Brazil. Mycopathologia 2006;161: 141–5.
[6] Casal M, Linares MJ, Solís F, Rodríguez FC. Appearance of colonies of Prototheca on CHROMagar Candida medium. Mycopathologia 1997;137:79–82.
[7] Moller A, Truyen U. Roesler U: Prototheca zopfii genotype 2—The causative agent of bovine protothecal mastitis? Vet Microbiol 2007;120:370–4. Short communication.
[8] Ueno R, Urano N, Suzuki M. Phylogeny of the non-photosynthetic green microalgal genus *Prototheca* (Trebouxiophyceae, Chlorophyta) and related taxa inferred from SSU and LSU ribosomal DNA partial sequence data. FEMS Microbiol Lett 2003;223:275–80.
[9] Yoshida E, Makimura K, Mirhendi H, Kaneko T, Hiruma M, Kasai T, et al. Rapid identification of Trichophyton tonsurans by specific PCR based on DNA sequences of nuclear ribosomal internal spacer (ITS) 1 region. J Dermatol Sci 2006;42:225–30.
[10] Zhang QF, Saqhai Maroof MA, Allard RW. Effects on adaptedness of variations in ribosomal DNA copy number in populations of wild barley (Hordeum vulgare spp. spontaneum). Proc Natl Acad Sci USA 1990;87:8741–5.

Masanobu Onozaki[a,b]
Koichi Makimura[b,*]
Atsuhiko Hasegawa[b]

[a]*Kanto Chemical Co., Inc., Marusan Bldg. 11-5, Nihonbashi Honcho, 3-Chome, Chuo-ku, Tokyo 103-0023, Japan*
[b]*Teikyo University Institute of Medical Mycology, 359 Otsuka, Hachioji, Tokyo 192-0395, Japan*

*Corresponding author. Tel.: +81 426 78 3256; fax: +81 426 78 256
E-mail address: makimura@main.teikyo-u.ac.jp (K. Makimura)

28 April 2008

doi:10.1016/j.jdermsci.2008.10.009

Letter to the Editor

Desmosome splitting is a primary ultrastructural change in the acantholysis of pemphigus

To the Editor,

Pemphigus comprises a group of autoimmune blistering diseases affecting the skin and/or mucous membranes [1]. The blister formation in pemphigus has been elucidated markedly and shown to be caused by autoantibodies against desmoglein 1 (Dsg 1) and desmoglein 3 (Dsg 3) [2]. On the other hand, morphological studies using electron microscope on pemphigus were performed in 1960s [3–5], when little was known about their underlying molecular pathophysiology. Now the changes of desmosome-keratin cytoskeleton have come to the central point of discussion as the cause of acantholysis, it is necessary and timely to re-evaluate the ultrastructural changes in pemphigus, particularly focusing to the changes of desmosomes and cytoskeletal structures.

Two mucocutaneous type pemphigus vulgaris (PV) cases, one mucosal-dominant PV case, and two pemphigus foliaceus (PF) cases (Table 1) were analyzed in this study. Skin biopsies were taken from the new blister on the skin or buccal mucous membrane. By light microscopy, acantholysis was clearly observed in all five cases and, in addition, spongiosis with lymphocytic infiltration was seen near the blister in two PV cases. By observing the acantholytic area by electron microscopy, half-split desmosomes were seen on the cell surface in all cases (Fig. 1A). In the acantholytic keratinocytes with fully developed blisters, keratin condensation around the cell nucleus resulted in the total disappearance of tonofilaments at cell periphery (Fig. 1B). We could not find any difference in the ultrastructural features between mucocutaneous type PV and mucosal-dominant type PV. In addition, we observed no differences in desmosomal change between PV and PF at high magnification.

The close chronological relationship between keratin retraction and half-split desmosome formation required further clarification. When focusing on apical cell surface of a basal cell in the very edge of a blister in PV, several stages of the half-split desmosomes were recognized (Fig. 1C–G). Where plasma membranes of basal and suprabasal cells were observed nearby, an initial stage of half-split desmosome was seen located on the protruded cell membrane with a thick and dense attachment plaque and abundant keratin filament insertion (Fig. 1D). As the cell detached, the keratin insertion decreased (Fig. 1E and F) and finally attachment plaque disappeared (Fig. 1G). These data imply that keratin retraction occurs after desmosomal split.

By observing the spongiotic area seen in two PV cases, enlargement of the extracellular space was seen in the epidermis, which could be regarded as shrinking of keratinocytes. Lymphocytic infiltration within the epidermis was almost always seen. No desmosomal split or keratin retraction was observed in the shrunken cells. Instead, desmosomes were observed between philopodial projections spanning two neighboring keratinocytes into a widened intercellular space (Fig. 1H). All these findings of spongiotic area were similar to those reported in allergic contact dermatitis caused by DNCB treatment in the normal human skin [6] and may not be specific to pemphigus.

From these results, we would like to stress three messages. First, there was no significant difference between PV and PF in terms of desmosomal split and keratin retraction. The difference of autoantibody profile is not crucial for the morphology of each desmosomal split. Second, desmosomal split always precede keratin retraction in vivo. Müller et al. [7] have indicated that autoantibody binding can induce keratin retraction independently to cell separation using cultured mouse keratinocytes. We have reported using immuno-electron microscopy on a PV model mouse that desmosomes on the apical surface of basal cells showed splits without keratin retraction and those on the lateral side showed

Cases	Sex	Age (years)	Skin lesion	Mucosal lesion	Suprabasilar acantholysis	Superficial acantholysis	Spongiosis	ELISA	
								Dsg 1	Dsg 3
PV1	M	57	+	+	+	–	–	62.9	136.8
PV2	F	58	+	+	+	–	+	104.7	113.2
mPV	F	40	–	+	+	–	+	20.0	260.7
PF1	M	55	+	–	–	+	–	80.6	2.2
PF2	M	32	+	–	–	+	–	139.0	0.7

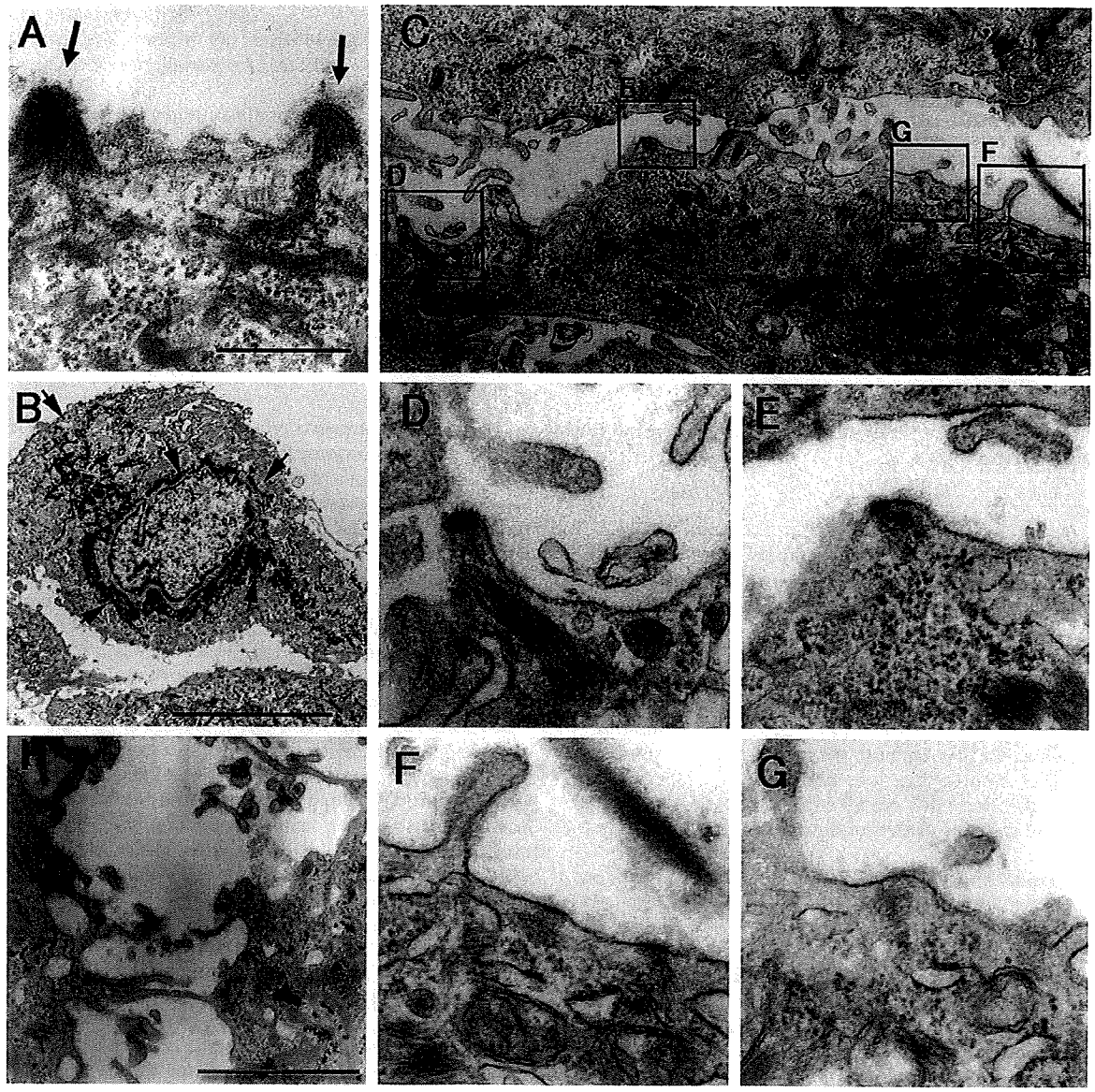

Fig. 1. (A) Half-split desmosomes (arrows) observed in the early stages of a lesion in PF. Scale bar = 500 nm. (B) Marked keratin retraction (arrows) was seen in the acantholytic cells of a PF case within the fully developed blister cavity. Scale bar = 5 μm. (C) Formation and degradation of half-split desmosomes in a PV case. Apical surface of a basal cell at the very edge of the blister in PV showed various stages of half-split desmosomes. The lower cell is a basal keratinocytes and upper cell is a suprabasal keratinocytes. Rectangles indicated the location of half-split desmosomes demonstrated below (D–G) in high power view. (D) At the initial stage, half-split desmosome was observed on the protruded cell surface and had a dense and thick attachment plaque with abundant keratin filament insertion (E) As cell membrane departed from the suprabasal cell, keratin insertion decreased and (F) attachment plaque became thinner. (G) Finally, rudimental attachment plaque was seen. (H) In the basal cell cytoplasm in areas of spongiosis, no keratin retraction was seen, but small vesicles and free ribosomes were observed. Normal desmosomes were seen in the widened intercellular space between the keratinocytes in mucocutaneous type of PV. Scale bars = 2 μm.

keratin retraction accompanied by loss of desmoplakin from the desmosome without splitting of the desmosome [8]. We assume that the apical desmosomes are more susceptible to mechanical stress rather than the lateral basal keratinocyte desmosomes, which are reinforced by rigidity of the basement membrane in vivo. The apical desmosome split may be triggered by mechanical force, which can be clinically described as Nikolsky phenomenon. This may be a reason why splitting of the desmosome is always accompanied by widened intercellular space, which may also occur by intercellular exudation of serum components. Perilesional epidermis showed various degree of detachment of non-desmosomal plasma membranes but this was not significantly different from that seen in the normal epidermis. Third, so-called basal cell shrinkage should be interpreted as a result of intercellular edema caused by inflammatory process of spongiosis, and not the cause of acantholysis. In this study, we have identified two patterns of cell separation; desmosomal split in all five cases and intercellular edema in two cases. Some papers have raised the hypothesis that changes in cytoskeletal structure induce the collapse and shrinkage of cells resulting in cell separation [9]. However, we could not find crucial changes in the cytokeratin during the shrinkage of basal cells. Moreover, these widening of extracellular spaces were not restricted between basal and suprabasal cells but seen in full thickness of the Malpigi layer of the epidermis in PV.

In summary, when desmosomal adhesive function is disrupted, splitting of the desmosome likely occurs after mechanical stress, and then keratin retraction follows in association with the disappearance of the half-split desmosome. When desmosomal function is insufficiently perturbed and inflammatory change predominates, intercellular edema occurs without desmosome split or keratin retraction. Both these features may co-exist at varying frequency in different regions. Although spongiosis is a part of characteristic histological feature of pemphigus, splitting of the desmosomal plaque is the primary ultrastructural change that accounts for the acantholysis in both pemphigus vulgaris and foliaceus.

Acknowledgement

This work was supported by a Grant-in Aid for Scientific Research from the Ministry of Education, Culture, Sports, Science and Technology of Japan.

References

[1] Stanley JR, Amagai M. Pemphigus, bullous impetigo, and the staphylococcal scalded-skin syndrome. N Engl J Med 2006;355:1800–10.
[2] Amagai M, Tsunoda K, Zillikens D, Nagai T, Nishikawa T. The clinical phenotype of pemphigus is defined by the anti-desmoglein autoantibody profile. J Am Acad Dermatol 1999;40:167–70.
[3] Hashimoto K, Lever WF. An electron microscopic study on pemphigus vulgaris of the mouth and the skin with special reference to the intercellular cement. J Invest Dermatol 1967;48:540–52
[4] Hashomoto K, Lever WF. The intercellular cement in pemphigus vulgaris, an electron microscopic study. Dermatologica 1967;135:27–34.
[5] Wilgram GF, Caulfield JB, Lever WF. An electron microscopic study of acantholysis in pemphigus vulgaris. J Invest Dermatol 1961;36:373–82
[6] Komura J, Ofuji S. Ultrastructural studies of allergic contact dermatitis in man. Epidermal cell changes at 3, 6, 12 h after application of DNCB. Arch Dermatol Res 1980;267:275–82.
[7] Muller EJ, Hunziker T, Suter MM. Keratin intermediate filament retraction is linked to plakoglobin-dependent signaling in pemphigus vulgaris. J Am Acad Dermatol 2007;56. 890-1-2.
[8] Shimizu A, Ishiko A, Ota T, Tsunoda K, Amagai M, Nishikawa T. IgG binds to desmoglein 3 in desmosomes and causes a desmosomal split without keratin retraction in a pemphigus mouse model. J Invest Dermatol 2004;122: 1145–53.
[9] Bystryn J-C, Grando SA. A novel explanation for acantholysis in pemphigus vulgaris: the basal cell shrinkage hypothesis. J Am Acad Dermatol 2006;54:513–6.

Wenqing Wang[a,b]
Masayuki Amagai[b]
Akira Ishiko[b,*]

[a]*Department of Dermatology, The fourth Affiliated Hospital of Hebei Medical University, Shijiazhuang, China*
[b]*Department of Dermatology, Keio University School of Medicine, Tokyo, Japan*

*Corresponding author at: Department of Dermatology, Keio University School of Medicine, 35 Shinanomachi, Shinjuku, Tokyo 160-8582, Japan. Tel.: +81 3 3353 1211; fax: +81 3 3353 6880
E-mail address: ishiko@sc.itc.keio.ac.jp (A. Ishiko)

doi:10.1016/j.jdermsci.2008.10.010

Letter to the Editor

Prevalence of obesity/adiposity in Japanese psoriasis patients: Adiposity is correlated with the severity of psoriasis

ARTICLE INFO

Keywords.
Body mass index
Disease activity
Percent body fat
Psoriasis
Visceral adiposity

Although epidemiologic survey revealed an association between psoriasis and obesity/adiposity [1], no reports are present on the relationship in Japanese psoriasis patients. Obesity induces overproduction of inflammatory cytokines such as tumor necrosis factor α (TNF-α), interleukin (IL)-6, and IL-8 in adipose tissue. The serum levels of TNF-α, IL-6, and IL-8 are increased in psoriasis and are associated with the disease severity [2]. Adipocytes also produce leptin, which acts primarily through the specific receptors at hypothalamus [3]. Leptin decreases appetite and increases energy expenditure and serum levels of leptin are known to reflect the body fat mass [3]. Adiponectin is another adipocyte-specific secretary protein abundantly present in circulation. Plasma levels of adiponectin are paradoxically decreased in obesity, insulin-resistance [4], and hypoadiponectinemia is closely associated with metabolic syndrome [5]. Recent study demonstrated that adiponectin and TNF-α suppress each other's production and also antagonize each other's function in their target cells [6]. We have shown the increased plasma leptin levels and decreased adiponectin levels in Japanese psoriasis patients [7].

Although the obesity or overweight usually means from increased fat of the body, there is some exception such as muscular athletes, and visceral adiposity persons who are within the normal range of body mass index (BMI). So we evaluated obesity/adiposity as.BMI, %BF, and visceral adiposity and used the obesity as the term estimated by BMI. Adiposity was used as the term estimated by %BF and visceral adiposity. The aim of the